

Synthesis and Characterization of Poly(vinylidene fluoride)-*g*-poly(styrene) Graft Polymers Obtained by Atom Transfer Radical Polymerization of Styrene

L. Sauguet, C. Boyer, B. Ameduri,* and B. Boutevin

Laboratory of Macromolecular Chemistry, UMR-CNRS 5076, Institute Gerhardt, Ecole Nationale Supérieure de Chimie de Montpellier, 8 rue de l'Ecole Normale, 34296 Montpellier Cedex 05, France

Received July 11, 2006; Revised Manuscript Received September 26, 2006

ABSTRACT: Poly(vinylidene fluoride)-*g*-poly(styrene) graft copolymers (PVDF-*g*-PS) were synthesized by the “grafting from” method from a PVDF macroinitiator bearing bromine side groups. This fluorinated macroinitiator was obtained from the radical copolymerization of VDF with 8-bromo-1*H*,1*H*,2*H*-perfluorooct-1-ene (BDFO), and then it was used in the atom transfer radical polymerization (ATRP) of styrene initiated by Cu^IBr/1,1,4,7-, 10,10-hexamethyltriethylenetetramine (HMTETA) catalyst. First, the synthesis of a model poly(styrene) was investigated starting from 1-bromoperfluorooctane (C₈F₁₇Br) as the initiator to check the reactivity of –CF₂–Br in ATRP process. Successful ATRP of styrene in the presence of 1-bromoperfluorooctane was observed from a kinetic study and NMR spectroscopy, and the activation rate constant of this initiator ($k_{\text{act}} = 35 \times 10^{-3} \text{ M}^{-1} \text{ s}^{-1}$ at 35 °C in acetonitrile) was assessed for the first time. In a second part, ATRP of styrene was also studied from poly(VDF-*co*-BDFO) copolymers as the macroinitiators, taking into account: (i) the effect of the polymerization temperature, (ii) the ligand concentration in the ATRP catalyst, and (iii) the amount of solvent vs the conversion of poly(styrene). The formation of graft copolymers was confirmed by size exclusion chromatography and by ¹H and ¹⁹F NMR spectroscopies. Interestingly, the linear dependences of both the evolutions of $\ln([M]_0/[M])$ vs time and of the molecular weights of the resulting graft copolymers vs the styrene conversions, and the decrease of their dispersity indexes vs the styrene conversions evidenced the controlled behavior of that graft polymerization.

Introduction

Graft copolymers are well-defined copolymers, that have already demonstrated relevant properties and hence have been used in many applications (such as emulsifiers for plastics, hot melt, adhesives, ions exchange membranes, impact resistance additives).^{1–3} It is well-known that heterogeneous (i.e., two phases or more) graft copolymers tend to show the properties of both (or more) polymeric backbone and the oligomeric or polymeric grafts rather than averaging the properties of both homopolymers. Among these copolymers, fluorinated graft copolymers⁴ have drawn great interest, since in the past decade the number of articles dealing with the synthesis, properties, and applications of fluorinated graft polymers has been increasing.

Poly(vinylidene fluoride)⁵ (PVDF) exhibits very interesting piezo and pyroelectrical properties, chemical inertness to acids and solvents (except DMF, DMSO, trifluorotoluene and dimethylacetamide), low permeability, and resistance to nuclear radiations that enables it to be used in many applications (loud speakers, piano keys, IR detectors, paints and coatings and in various fields of mining, food, biomedical and engineering industries). In addition, PVDF is not toxic and less expensive than other fluoropolymers such as poly(chlorotrifluoroethylene), poly(trifluoroethylene) or poly(tetrafluoroethylene). Thus, graft copolymers containing a PVDF backbone would be particularly interesting, and potentially useful, because the incorporation of PVDF would raise the chemical resistance and thermal stability of the polymer and should lower the surface energy.

Basically, three different methods enable one to synthesize fluorinated graft copolymers, recently summarized:⁴ the “graft-

ing through”,^{6–8} the “grafting from”, and the “grafting onto” routes. The second method seems to be the most used, especially by two main strategies: (i) by the irradiation (plasma, swift heavy ions, X-rays, or electron beam, mainly under γ rays or ⁶⁰Co source) of fluoropolymers followed by a grafting (that strategy was extensively used by Holmberg et al.⁹ who synthesized PVDF-*g*-poly(styrene sulfonic acid) graft copolymers for fuel cell membranes); (ii) by transfer to the polymer;¹⁰ (iii) by ozonization of PVDF;¹¹ (iv) by the direct terpolymerization of two fluoroalkenes such as VDF and chlorotrifluoroethylene (CTFE) with *tert*-butylallyl peroxycarbonate at low temperature leading to terpolymers bearing peroxycarbonate¹² dangling groups. Hence, these original macroinitiators were able to initiate the radical polymerization of VDF to yield poly(VDF-*co*-CTFE)-*g*-PVDF graft copolymers¹² as original thermoplastic elastomers. However, these above methods did not allow to assess the molecular weights of the graft segments.

To avoid this drawback, the controlled radical polymerization was used and has become one of the most useful strategies for the synthesis of graft polymers¹³ while this technique was also successful in achieving fluorinated block copolymers^{4,14–20} from initiators containing C–I, C–Br, and C–Cl bonds. For examples, Chen et al.²¹ and Ying et al.²² reported the synthesis of graft copolymer by reversible addition–fragmentation chain transfer polymerization (RAFT) to obtain original PVDF-*g*-PMMA and PVDF-*g*-poly(acrylic acid) (PVDF-*g*-PAA) graft copolymers. Yin et al.²² prepared PVDF-*g*-PAA and PVDF-*g*-PAA-*b*-PNIPAAm copolymers by RAFT polymerization of acrylic acid with a ozone-pretreated PVDF.

ATRP was also used to control the graft segments. Indeed, ATRP²³ is regarded as one of the most efficient controlled (or pseudo-living) polymerization methods to prepare polymers and copolymers endowed with different architectures and low

* Corresponding author. Telephone: +33-467-144-368. Fax +33-467-147-220. E-mail: bruno.ameduri@enscm.fr.

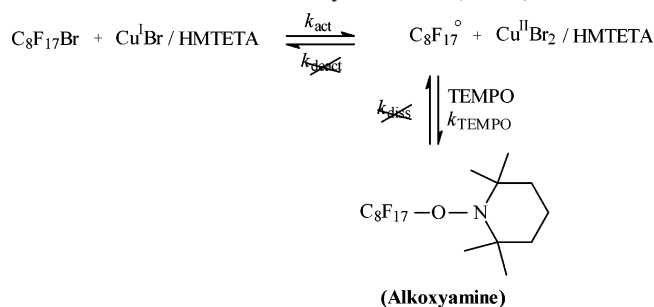
polydispersities.^{24–27} To the best of our knowledge, Inceoglu et al.,²⁸ Chen et al.^{29–31} and Hester et al.³² synthesized different graft copolymers of PVDF, such as poly(vinylidene fluoride)-*g*-poly(methyl methacrylate) (PVDF-*g*-PMMA) or poly(vinylidene fluoride)-*g*-poly(oxyethylene methacrylate) (PVDF-*g*-POEM) graft copolymers by ATRP of various methacrylates from PVDF. Surprisingly, these studies used the presence of C–F bond on the polymeric chain of PVDF to initiate the ATRP polymerization. More recently, Zhang and Russel³³ reported another method of grafting poly(styrene) and poly(*tert*-butyl acrylate) from poly(vinylidene fluoride-*co*-chlorotrifluoroethylene) (poly(VDF-*co*-CTFE)) random copolymers via ATRP. Indeed, such a controlled “grafting from” method has been possible via the C–Cl bond (from CTFE units in poly(VDF-*co*-CTFE) statistic polymers) but, to our knowledge, the literature does not report any investigation from polymers bearing C–Br side groups to enable ATRP. However, we have recently achieved the synthesis of PVDF containing –C₆F₁₂Br dangling groups.³⁴ Interestingly, these C–Br side-bonds may offer a possible cleavage under radical conditions. Hence, the objectives of this article deal with the synthesis and the characterization of PVDF-*g*-PS graft copolymers where PS stands for poly(styrene) from the ATRP of styrene with poly(VDF-*co*-8-bromo-1*H*,1*H*,2*H*-perfluorooct-1-ene), poly(VDF-*co*-BDFO) copolymers, as original macroinitiators. First, it was of interest to study the ATRP of styrene from C₈F₁₇Br as a model initiator in term of radical polymerization (i.e., to investigate its controlled character and the narrow polydispersity indexes (PDI) of the produced C₈F₁₇–PS). The choice of this model molecule can be explained by the similar structure of the end group of C₈F₁₇Br with –CF₂Br dangling groups borne by poly(VDF-*co*-BDFO) copolymers. Then, the experimental conditions of this model reaction have been extended onto original copolymers based on VDF units and bearing perfluorobrominated side groups. In addition, a preliminary kinetics of ATRP of styrene for the synthesis of PVDF-*g*-PS graft copolymers from poly(PVDF-*co*-BDFO) copolymer as the macroinitiator has also been attempted.

Experimental Part

Materials. Cu^IBr, 1,1,4,7,10,10-hexamethyltriethylenetetramine (HMTETA), 2,2,6,6-tetramethylpiperidiny-1-oxy (TEMPO, 99%, purified by sublimation), and styrene were purchased from Aldrich Chimie (Saint Quentin-Fallavier, France). Cu^IBr was washed with glacial acetic acid to remove any soluble oxidized species, filtered, washed with ethanol and dried under vacuum. Styrene was distilled over CaH₂ and HMTETA was used as received. 1-Bromoperfluorooctane was kindly offered by Atofina (Pierre Benite, France). Dimethylformamide (DMF, 99%), dimethylacetamide (DMAc), tetrahydrofuran (THF, 99%), acetonitrile (99.7%), and methanol (99.8%) provided from SDS (Peypin, France), were used as received. Poly(VDF-*co*-BDFO) copolymers were synthesized by radical copolymerization of vinylidene fluoride (VDF) with 8-bromo-1*H*,1*H*,2*H*-perfluorooct-1-ene (BDFO) described in the Supporting Information.

Analyses. Poly(styrene) and PVDF-*g*-PS aliquots, sampled from the reactional medium, were characterized by ¹H NMR (250 or 400 MHz) and ¹⁹F (200 or 400 MHz) spectroscopies. The NMR spectra were recorded on Bruker AC 200, AC 250 and AC 400 instruments, using deuterated acetone or chloroform as the solvents and tetramethylsilane (TMS) (or CFCl₃) as the references for ¹H (or ¹⁹F) nuclei, respectively. Coupling constants and chemical shifts are given in Hz and ppm, respectively. The experimental conditions for recording ¹H (or ¹⁹F) NMR spectra were as follows: flip angle 90° (or 30°), acquisition time 4.5 s (or 0.7 s), pulse delay 2 s (or 5 s), number of scans 16 (or 64), and a pulse width of 5 μs for ¹⁹F NMR.

Scheme 1. Kinetics Isolation of the Activation Process in Atom Transfer Radical Polymerization (ATRP)^a



^a k_{act} , k_{deact} , TEMPO, k_{TEMPO} and HMTETA stand for activation rate constant, deactivation rate constant, 2,2,6,6-tetramethylpiperidiny-1-oxy, rate constant for radical coupling between radical and TEMPO, 1,1,4,7,10,10-hexamethyltriethylenetetramine, respectively.

Size exclusion chromatography (SEC) was performed at 30 °C on a Spectra-Physics apparatus with three PL gel 5 μm MIXED-D columns, 500 Å, and 100 Å from Polymer Laboratories, and equipped with two detectors: Shodex refractive index and UV. THF was used as the solvent at 0.8 mL min^{−1}. The calibration was established with poly(styrene) standards from Polymer Laboratories.

Gas chromatography analyses (GC) were carried out on a Delsi Instruments Serial 330 apparatus coupled with a Shimadzu C-R6A integrator. A 2 m long Carbowax 20 M (poly(ethylene glycol)) column was used with nitrogen as the gas vector at 1 bar. The analyses were achieved in an isothermal mode at 130 °C (at $T_{injector}$ = 130 °C and T_{detect} = 200 °C). GC enabled us to determine the monomer conversion vs reaction time by means of the solvent (generally DMF) as the internal standard.

The matrix-assisted laser desorption–ionization time-of-flight mass spectrometric (MALDI–TOF–MS) analyses were executed at “Ultraflex Bruker” (Université Montpellier II) in reflection mode (accelerating potential of 20 kV) on a Bruker apparatus equipped with a nitrogen laser (337 nm). 2,3,4,5,6-Pentafluorocinnamic acid (PFCA) and sodium iodide were used as the matrix and as the cationizing agent, respectively. The concentrations of sample and matrix solutions were 10 g L^{−1} (in THF), while the analyte/matrix ratio was 1/10 v/v. Then, 1 μL of the mixture was deposited on a stainless steel target, air-dried, and introduced in the spectrometer under vacuum.

Thermogravimetric analyses (TGA) were performed with a TGA/SDTA 851 thermobalance from Mettler DAL 75965 and Lauda RC6 CS cryostat apparatus, under air, at the heating rate of 5 °C·min^{−1} from room temperature up to a maximum of 580 °C.

Differential scanning calorimetry (DSC) measurements were conducted using a TA 2920 analyzer from TA Instruments DA 73085, a RCS DA cooler, and Sartorius MC5 weighing machine. Scans were recorded at a heating rate of 20 °C·min^{−1} from −100 to +100 °C, and the cooling rate was 20 °C·min^{−1}. A second scan was required for the assessment of the T_g , defined as the inflection point in the heat capacity jump.

Assessment of the Activation Rate Constant Measurements.^{23,35–46}

The activation rate constants were determined using the trapping experiments that were also used for the determination of the dissociation rate parameters of alkoxyamines.⁴⁷ The radicals arising from the homolytic halogen abstraction from the alkyl halides were irreversibly trapped by a stable nitroxide radical, such as 2,2,6,6-tetramethylpiperidiny-1-oxy (TEMPO), to yield the corresponding alkoxyamines (Scheme 1).⁴⁸ This was achieved by using a large excess of TEMPO (ca. 10 times) with respect to alkyl halides. This process was also made easier due to a higher rate constant for radical coupling than that of deactivation ($k_{TEMPO} \gg k_{deact}$).⁴⁸ An excess of Cu^I species (ca. 20 times about alkyl halide) was used to carry out the kinetics straightforward, i.e., to provide pseudo-first-order kinetic conditions (Scheme 1). The apparent (k_{app}) and activation (k_{act}) rate constants were assessed from the slope of the pseudo-first-order plots (eq 1). Thus, the slopes of the straight lines should follow externally first-order dependence in respect to [Cu^I]₀ (as shown in

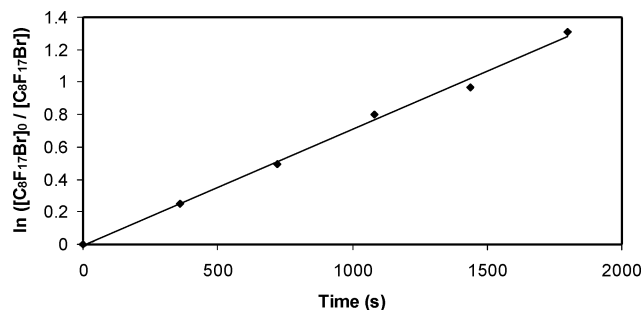


Figure 1. Pseudo-first-order kinetics plot of the activation process for 1-bromoperfluorooctane ($C_8F_{17}Br$) used as initiator with $Cu^I Br/HMTETA$ catalytic system in acetonitrile at 35 °C. $[Cu^I Br]_0/[C_8F_{17}Br]_0/[HMTETA]_0 = 20:1:10:20$. HMTETA stands for 1,1,4,7,10,10-hexamethyltriethylenetetramine. Experimental conditions: 0.143 g (1×10^{-3} mol) of copper bromide, 0.230 g (1×10^{-3} mol) of HMTETA, 0.025 g (5×10^{-5} mol) of $C_8F_{17}Br$, 0.080 g (5×10^{-4} mol) of 2,2,6,6-tetramethylpiperidinyl-1-oxy (TEMPO), and acetonitrile (50 mL) were placed into a dry round-bottom flask at 35 °C.

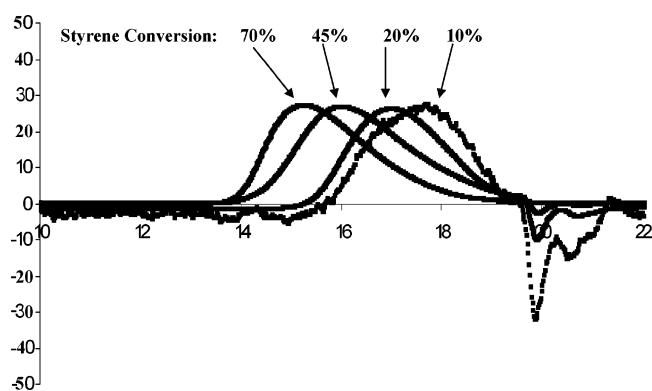


Figure 2. Evolution of the size exclusion chromatography (SEC) traces of the resulting polymers at different styrene conversions for the ATRP of styrene using $C_8F_{17}Br$ as the initiator. Experimental conditions: $[C_8F_{17}Br]_0/[styrene]_0/[Cu^I Br]_0/[HMTETA]_0 = 1.0:100.0:1.0:1.0$ in DMF at 110 °C; copper bromide (28.6 mg, 2×10^{-4} mol), 1,1,4,7,10,10-hexamethyltriethylenetetramine (HMTETA) (46.6 mg, 2×10^{-4} mol), $C_8F_{17}Br$ (0.10 g, 2×10^{-4} mol), and styrene (2.08 g, 2×10^{-2} mol) and 10.0 g of dimethylformamide (DMF); experiment no. 5 in Table 1.

Figure 1). The initial concentration of Cu^I species ($[Cu^I Br/HMTETA]_0$) enabled us to calculate k_{app} , whereas the concentration of active Cu^I species ($[Cu^I Br/HMTETA]_{act}$) was used to determine k_{act} because $[Cu^I Br/HMTETA]_{act}$ could be different from $[Cu^I Br/HMTETA]_0$, especially in less polar solvents⁴⁶ but not in the case of acetonitrile.^{23,35–46} However, the activation rate constant, k_{act} , should be constant and independent from $[Cu^I Br/HMTETA]_{act}$. To obtain pseudo-first-order kinetics, the following condition was required and the activation rate constant (k_{act}) was assessed from the slope of the pseudo-first-order plot.

pseudo first order $[Cu^I Br]_0/[HMTETA]_0 \gg [C_8F_{17}Br]_0$

$$\frac{-d \ln [C_8F_{17}Br]}{dt} = \text{slope} = k_{app} [Cu^I Br/HMTETA]_0 = k_{act} [Cu^I Br/HMTETA]_{act} \quad (1)$$

$$k_{act} = 35 \times 10^{-3} \text{ mol}^{-1} \text{ s}^{-1} \text{ at } 35 \text{ °C in acetonitrile}$$

General Procedure for the Assessment of the Activation Rate Constant in Acetonitrile at 35 °C (with Initial Molar Ratio $[Cu^I Br]_0/[C_8F_{17}Br]_0/[TEMPO]_0/[HMTETA]_0 = 20:1:10:20$). Freshly purified and dried copper bromide (0.143 g, 1×10^{-3} mol), 1,1,4,7,10,10-hexamethyltriethylenetetramine (HMTETA) (0.230 g, 1×10^{-3} mol), $C_8F_{17}Br$ (0.025 g, 5×10^{-5} mol), 2,2,6,6-

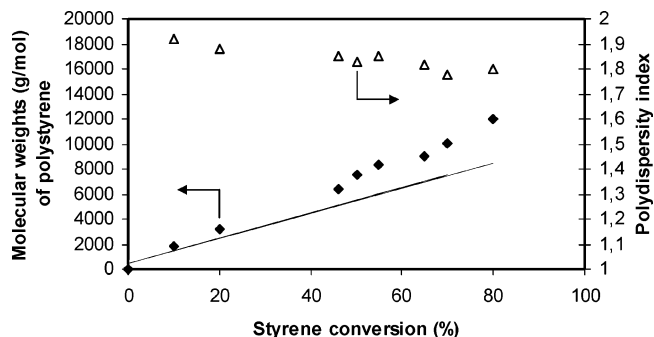


Figure 3. Dependence of molecular weight (\blacklozenge) and polydispersity index (Δ) of poly(styrene) vs styrene conversion for the ATRP of styrene in the presence of $C_8F_{17}Br$ as the initiator. The full line represents the theoretical curve. Experimental conditions: $[C_8F_{17}Br]_0/[styrene]_0/[Cu^I Br]_0/[HMTETA]_0 = 1.0:100.0:1.0:1.0$ at 110 °C; copper bromide (28.6 mg, 2×10^{-4} mol), 1,1,4,7,10,10-hexamethyltriethylenetetramine (HMTETA) (46.6 mg, 2×10^{-4} mol), $C_8F_{17}Br$ (0.10 g, 2×10^{-4} mol), and styrene (2.08 g, 2×10^{-2} mol) and 10.0 g of dimethylformamide (DMF); experiment no. 5 in Table 1.

tetramethylpiperidinyl-1-oxy (TEMPO) (0.080 g, 5×10^{-4} mol), and acetonitrile (50 mL) were placed into a dry round-bottom flask. The mixture was purged with nitrogen and then stirred in an oil bath at 35 °C. The conversion of $C_8F_{17}Br$ was monitored by ^{19}F NMR, and the activation rate constant, k_{act} , was assessed as reported above.

$$\alpha(C_8F_{17}Br) = 1 - [(3 \times \int (-CF_2Br) (-60.0 \text{ ppm})) / (2 \times \int (-CF_3) (-82.0 \text{ ppm}))] \quad (2)$$

with $\alpha(C_8F_{17}Br)$, $\int(-CF_2Br)$ and $\int(-CF_3)$ standing for $C_8F_{17}Br$ conversion, integral of $-CF_2Br$, and integral of $-CF_3$, respectively.

$$\ln[C_8F_{17}Br]_0/[C_8F_{17}Br] = -\ln(1 - \alpha(C_8F_{17}Br)) \quad (3)$$

General Procedure for the Radical Polymerization of Styrene with $C_8F_{17}Br$ as the Initiator (with Initial Molar Ratio $[C_8F_{17}Br]_0/[styrene]_0/[Cu^I Br]_0/[HMTETA]_0 = 10:100:1:1$). Freshly purified and dried copper bromide (28.6 mg, 2×10^{-4} mol), 1,1,4,7,10,10-hexamethyltriethylenetetramine (HMTETA) (46.6 mg, 2×10^{-4} mol), $C_8F_{17}Br$ (1.002 g, 2×10^{-3} mol), freshly distilled styrene (2.080 g, 2×10^{-2} mol), and the solvent (DMF or DMAc) were placed into a dry round-bottom flask. The mixture was purged with nitrogen and then stirred in an oil bath at 110 °C. The progress of the reaction was monitored by 1H and ^{19}F NMR and GC and SEC chromatographies. At the end of the reaction, the mixture was filtered through a short column of silica gel (diameter, 10 mm; length, 30 mm) to remove the catalyst. The polymer was then precipitated from methanol, filtered, and dried at 60 °C under vacuum for 16 h.

^{19}F NMR (acetone- d_6 , ppm, δ , Figure 5): -80.6 (m, $CF_3-CF_2-C_6F_{12}-(Sty)_n-Br$, 3F); -112.4 (m, $C_6F_{13}-CF_2-CF_2-(Sty)_n-Br$, 2F); -121.5 (m, $C_6F_{13}-CF_2-CF_2-(Sty)_n-Br$, 2F); -121.8 ($C_4F_9-CF_2-CF_2-C_2F_4-(Sty)_n-Br$, 4F); -122.6 (m, $C_3F_7-CF_2-CF_2-C_3F_6-(Sty)_n-Br$, 2F); -123.5 (m, $C_2F_5-CF_2-CF_2-C_4F_8-(Sty)_n-Br$, 2F); -126.0 (m, $CF_3-CF_2-CF_2-C_5F_{10}-(Sty)_n-Br$, 2F).

1H NMR (acetone- d_6 , ppm, δ , Figure 4): 1.2–1.6 (methylene groups of poly(styrene), $2H \times n$, with n corresponding to the number of styrene units); 1.8–2.1 (methyne groups adjacent to aromatic ring in poly(styrene), $1H \times n$); 2.5–2.8 ($R-CF_2-CH_2-CH(C_6H_5)-$, 2H); 4.2–4.7 ($-CH(C_6H_5)Br$, $1H \times n$); 6.5–7.4 (aryl protons of poly(styrene), $5H \times n$).

MALDI-TOF-MS (Figure 6).

Synthesis of 8-Bromo-1H,1H,2H,2H-perfluorooct-1-ene. In a round-bottom flask equipped with a condenser, 50.0 g (0.102 mol) of 1,8-dibromo-1H,1H,2H,2H-perfluorooctane diluted with ethanol was dropwise added in a mixture composed of KOH in ethanol. After the addition at room temperature, the expected unsaturated

Table 1. Summary of the Targeted, Theoretical and Experimental Molecular Weights, Conversions and Polydispersity Indexes of the Polymers Obtained by Atom Transfer Radical Polymerization (ATRP) of Styrene in the Presence of Cu^IBr/1,1,4,7,10,10-Hexamethyltriethylenetetramine (HMTETA) as the Catalytic System and 1-Bromoperfluorooctane (C₈F₁₇Br) as the Initiator at 110 °C

expt no.	solvent	[C ₈ F ₁₇ Br] ₀ : [styrene] ₀ : [Cu ^I Br] ₀ : [HMTETA] ₀	time (h)	targeted M_n (g mol ⁻¹)	α^a (%)	theor M_n^b (g mol ⁻¹)	exptl M_n^c (g mol ⁻¹)	PDI ^c
1a	DMF	10.0:100.0:0:0	6.0	1500	05	—	45 000	2.9
1b	DMF	0.0:100.0:1.0:1.0	6.0	1500	06	—	40 000	2.7
1c	DMF	10.0:100.0:1.0:1.0	3.5	1500	60	1100	1800	1.6
2	DMAc	10.0:100.0:1.0:1.0	4.5	1500	70	1200	1900	1.4
3	DMF	3.3:100.0:1.0:1.0	5.0	3500	85	2980	4300	1.7
4	DMAc	3.0:100.0:1.0:1.0	4.0	3800	55	2550	3500	1.5
5	DMF	1.0:100.0:1.0:1.0	4.5	10 500	80	8500	12 000	1.8
6	DMAc	1.0:100.0:1.0:1.0	4.0	10 500	70	7500	9500	1.5

^a Conversion of monomer assessed by gas chromatography. ^b Targeted molecular weights determined by $M_n = (\alpha \times [\text{styrene}]_0) / [\text{C}_8\text{F}_{17}\text{Br}]_0 \times M_{\text{styrene}} + M_{\text{C}_8\text{F}_{17}\text{Br}}$, where α , $[\text{styrene}]_0$, and $[\text{C}_8\text{F}_{17}\text{Br}]_0$ represent the styrene conversion and the concentrations of styrene and of 1-bromoperfluorooctane (C₈F₁₇Br), respectively. ^c Molecular weights and polydispersity indexes measured by size exclusion chromatography (with Polystyrene standards).

product was distilled under vacuum (bp = 48 °C/20 mmHg). 33.0 g (0.081 mol) of a colorless liquid were obtained (yield = 79%). The purity of the product was checked by ¹H, ¹⁹F, and ¹³C NMR spectroscopies (see Figures 1–3 in the Supporting Information, respectively), mass spectroscopy, and gas chromatography.

8-Bromo-1H,1H,2H-perfluorooct-1-ene. CH₂=CH–CF₂–CF₂–CF₂–CF₂–CF₂–CF₂–Br: ¹⁹F NMR (acetone-*d*₆, ppm, δ): –64.5 (t, Br–CF₂–C₅F₁₀–CH=CH₂, ³J_{FF} = 14.0 Hz, 2F); –113.7 (m, Br–R_f–CF₂–CH=CH₂, 2F); –117.3 (m, Br–C₄F₈–CF₂–CF₂–CH=CH₂, 2F); –121.2 (m, Br–C₂F₄–CF₂–CF₂–CF₂–CH=CH₂, 4F); –123.5 (m, Br–CF₂–CF₂–C₄F₈–CH=CH₂, 2F).

¹H NMR (acetone-*d*₆, ppm, δ): 6.1 (m, Br–C₆F₁₂–CH=CH₂, 3H).

¹³C NMR (acetone-*d*₆, ppm, δ): 108 to 122 (tt, ¹J_{CF} = 312.6 Hz, ²J_{CF} = 37.4 Hz, assigned to the different CF₂ groups of the perfluorinated chain); 125.5 (t, Br–C₅F₁₀–CF₂–CH=CH₂, ²J_{CF} = 23.3 Hz); 127.4 (t, Br–C₆F₁₂–CH=CH₂, ³J_{CF} = 9.9 Hz).

Radical Copolymerization of Vinylidene Fluoride (VDF) with 8-Bromo-1H,1H,2H-perfluorooct-1-ene (BDFO). The radical copolymerizations of VDF with BDFO were performed in a 160 mL Hastelloy autoclave Parr System, equipped with a manometer, a rupture disk, inlet and outlet valves, and a mechanical anchor. An electronic system regulated and controlled the mechanical stirring and the heating in the autoclave. The autoclave was left closed for 20 min and purged with 30 bar of nitrogen pressure to prevent any leakage, degassed, and put under vacuum. Then, 1.33 g (4.1 × 10⁻³ mol) of 2,5-bis(*tert*-butylperoxy)-2,5-dimethylhexane (DHBP), 12.67 g (0.0311 mol) of BDFO, and 80 g of 1,1,1,3,3-pentafluorobutane were successively introduced. Afterward, 19.70 g (0.3078 mol) of VDF were introduced (checked by double weighing). The autoclave was then progressively heated to 135 °C, that temperature being maintained for 7 h. After reaction, the autoclave was cooled to room temperature and then put in an ice bath for 30 min. After unreacted VDF monomer was degassed, the vessel was opened. 1,1,1,3,3-Pentafluorobutane was evaporated and the poly(VDF-*co*-BDFO) copolymer formed was solubilized in acetone and precipitated from cold pentane. The polymer was filtered off, washed, and dried under vacuum (yield = 50%) and the resulting brown fine powder was characterized by ¹⁹F and ¹H NMR spectroscopies (Table 1 and Figures 4 and 5 in the Supporting Information, respectively).

General Procedure for the Synthesis of Graft Copolymers in the Presence of PVDF-*co*-BDFO as the Macroinitiator by ATRP (with Initial Molar Ratio [Br]₀: [Styrene]₀: [Cu^IBr]₀: [HMTETA]₀ = 5:100: 0.5:0.5). Freshly purified and dried copper bromide (28.6 mg, 2 × 10⁻⁴ mol), 1,1,4,7,10,10-hexamethyltriethylenetetramine (HMTETA) (46.6 mg, 2 × 10⁻⁴ mol), PVDF-*co*-BDFO copolymer (M_n = 15 000 g mol⁻¹ and PDI = 2.3, experiment no. 8 in Table 3, determined by SEC with poly(styrene) standards) (4.2 g, 2 × 10⁻³ mol) and freshly distilled styrene (4.16 g, 4 × 10⁻² mol) were placed into a dry round-bottom flask. The mixture was purged with nitrogen and then stirred in an oil bath at 110 °C. The progress of the reaction was monitored by ¹H and ¹⁹F NMR

and GC and SEC chromatographies. At the end of the reaction, the mixture was filtered through a short column of silica gel (diameter, 10 mm; length, 30 mm) to remove the catalyst. The polymer was then precipitated from methanol, filtered, and dried at 60 °C under vacuum for 16 h.

¹⁹F NMR (acetone-*d*₆, ppm, δ , Figure 10): –91.4 (–CH₂–CF₂–CH₂–, 2F); –94.8 (–(CH₂–CF₂)–[CH₂–CH(C₆F₁₂–(Sty)_{*n*}–Br)], 2F); from –112.4 to –124.0 ppm (m, –C₆F₁₂–(Sty)_{*n*}–Br, 12F, and –(CH₂CF₂)–(CF₂–CH₂)–(CH₂CF₂)–).

¹H NMR (acetone-*d*₆, ppm, δ , Figure 9): 1.2–1.6 ppm (methylene group of poly(styrene), 2H); 1.8–2.1 ppm (methyne groups adjacent to aromatic ring in poly(styrene), 1H); 2.5–2.8 (R_f–CF₂–CH₂–CH(C₆H₅)–, 2H) and (–(CH₂CF₂)–(CF₂–CH₂)–(CH₂–CF₂)–); 3.0 ppm (–(CH₂CF₂)–(CH₂–CF₂)–); (4.2–4.7 ppm (–CH(C₆H₅)Br, 1H × *n*, where *n* corresponds to the number of styrene units); 6.5–7.4 (aromatic protons of poly(styrene), 5H × *n*).

DSC (Figure 11): T_{g1} = –25 °C; T_{g2} = +88 °C.

TGA (under air) Figure 12.

Results and Discussion

(1) Model Reaction : ATRP of Styrene with 1-Bromoperfluorooctane (C₈F₁₇Br). The model polymerizations of styrene by atom transfer radical polymerization (ATRP) using C₈F₁₇Br as the initiator were performed at 110 °C in the presence of Cu^IBr/1,1,4,7,10,10-hexamethyltriethylenetetramine (HMTETA) as the catalyst in dimethylformamide (DMF) or dimethylacetamide (DMAc) as the solvents (Scheme 2). Both solvents were used to improve both the solubilities of all the reactants for that ATRP system and the efficiency on the polymerization of styrene.

Preliminary reactions were carried out with an initial molar ratio $R_0 = [\text{C}_8\text{F}_{17}\text{Br}]_0 / [\text{styrene}]_0$ ranging from 0.033 to 0.100. After reaction, the total product mixture was characterized by SEC and ¹H NMR and ¹⁹F NMR spectroscopy. Results are summarized in Table 1.

As expected, the molecular weights of the obtained poly(styrene)s directly depend on the initial amount of the brominated initiator (C₈F₁₇Br). This observation is in agreement with the regular ATRP mechanism proposed in Schemes 2 and 3. Nevertheless, Table 1 shows that the experimental values are higher than the theoretical ones and the lower the initial molar ratio, r_0 , the higher the difference between theoretical and experimental molecular weights. DMAc was the best solvent to solubilize the ATRP system and in the control of the molecular weights even if conversions were still low (60%). The poor agreement between experimental and theoretical molecular weights and the high polydispersity indexes are not common in controlled radical polymerization. This observation may arise from the difference of reactivity between –CF₂–Br of the initiator and –CH₂–CH(C₆H₅)–Br (of the end-capped

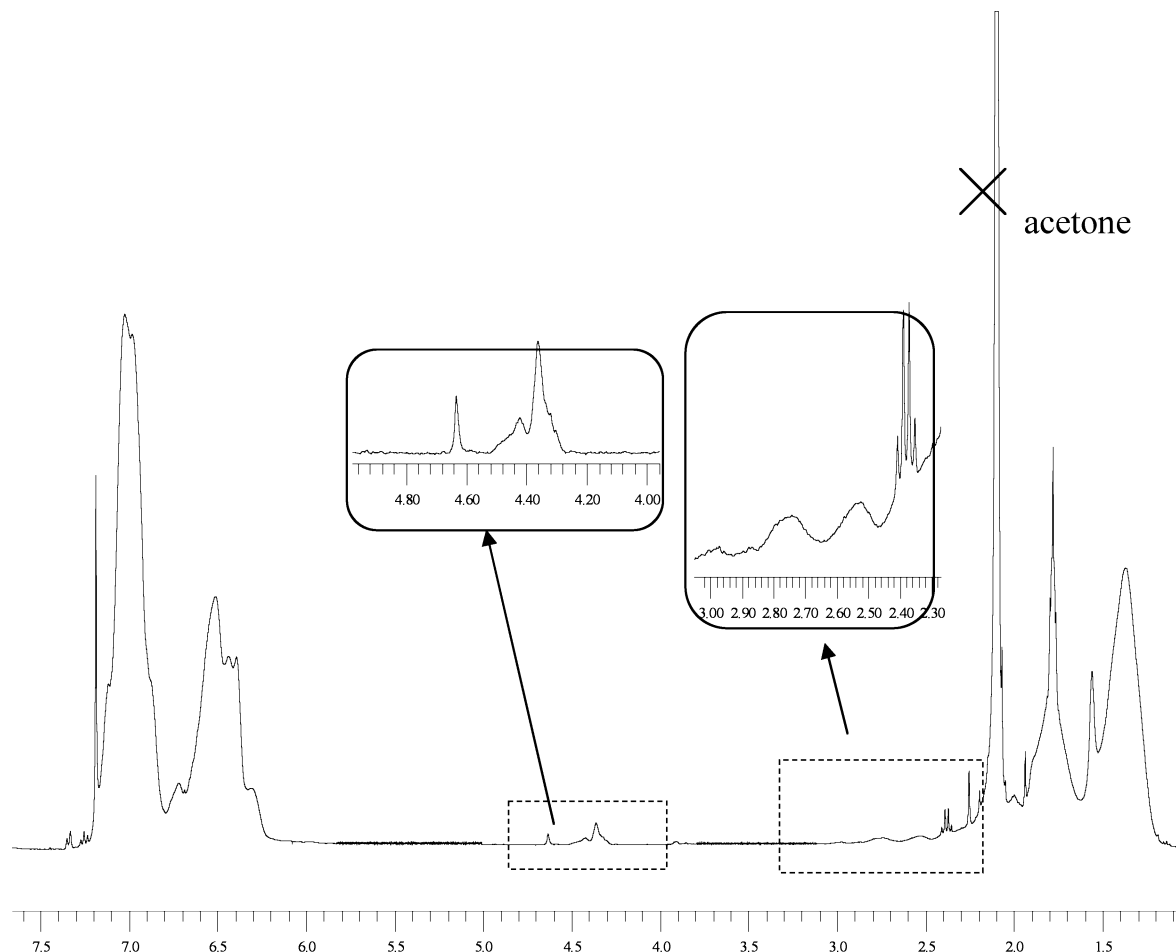


Figure 4. ^1H NMR spectrum of C_8F_{17} -poly(styrene) synthesized by ATRP using $\text{C}_8\text{F}_{17}\text{Br}$ as the initiator (recorded in deuterated acetone) (experiment no. 3, Table 1). Experimental conditions: $[\text{C}_8\text{F}_{17}\text{Br}]_0:[\text{styrene}]_0:[\text{Cu}^{\text{I}}\text{Br}]_0:[\text{HMTETA}]_0 = 3.3:100.0:1.0:1.0$; copper bromide (28.6 mg, 2×10^{-4} mol), 1,1,4,7,10,10-hexamethyltriethylenetetramine (HMTETA) (46.6 mg, 2×10^{-4} mol), $\text{C}_8\text{F}_{17}\text{Br}$ (0.33 g, 6.67×10^{-4} mol), and styrene (2.08 g, 2×10^{-2} mol) and 10.00 g of DMF.

intermediate) end groups. Without any catalytic complex or initiator in the reaction mixture (experiment nos. 1a and 1b in Table 1), the styrene conversion was low, and this can be explained by the thermal polymerization of styrene.

The mechanism of ATRP proposed in Scheme 3 is indeed a multistep mechanism: to obtain a good control of that ATRP, $\text{C}_8\text{F}_{17}\text{Br}$ initiator has to be more reactive than the obtained oligomers, $\text{C}_8\text{F}_{17}-[\text{CH}_2-\text{CH}(\text{C}_6\text{H}_5)]_n-\text{Br}$. Thus, the assessment of the activation rate constant (k_{act}) was required to establish the reactivity of the initiator.

Assessment of the Activation Rate Constant (k_{act}). The activation rate constant (k_{act}) was assessed in acetonitrile in the presence of both $\text{Cu}^{\text{I}}\text{Br}$ and HMTETA at 35 °C as described in the Experimental Section (Scheme 1). Acetonitrile is not regarded as a common solvent for ATRP but was used to obtain homogeneous catalyst solutions of the system and to compare the measured rate constant to those reported in the literature. The low temperature of reaction was necessary to avoid the dissociation of the C_8F_{17} -TEMPO species. Initial molar ratios of reactants were fixed at $[\text{Cu}^{\text{I}}\text{Br}]_0:[\text{C}_8\text{F}_{17}\text{Br}]_0:[\text{TEMPO}]_0:[\text{HMTETA}]_0 = 20:1:10:20$. The results are summarized in Table 2. Monitoring the consumption of the initiator (decrease of the signal located at -65 ppm assigned to difluoromethylene group in $\text{C}_7\text{F}_{15}-\text{CF}_2-\text{Br}$) vs time, we assessed the value of the activation rate constant, k_{act} (the details are reported in the experimental part). The activation rate constant for this system is $k_{\text{act}} = 35 \times 10^{-3} \text{ mol}^{-1} \cdot \text{s}^{-1}$ at 35 °C in acetonitrile.

This result was compared to those among the most widely used initiators of ATRP⁴⁸ (Table 2). Three alkyl halides were chosen for comparison: ethyl 2-bromoisobutyrate (EBriB), methyl 2-bromopropionate (MBrP), and 1-phenylethyl bromide (PEBr). This last one is the model compound for a polymeric chain end commonly used in ATRP of poly(styrene).²³

The decreasing order of the activation rate constants with $\text{CuBr}/N,N,N',N'$ -pentamethyldiethylenetetramine (PMDETA) or 1,1,4,7,10,10-hexamethyltriethylenetetramine (HMTETA) was: $\text{EBriB} \gg \text{PEBr} \geq \text{MBrP} \gg \text{C}_8\text{F}_{17}\text{Br}$ (Table 2). EBriB activates ATRP of styrene very fast with an activation rate constant ca. 10 times higher than those of PEBR and MBrP and 50 times greater than that of $\text{C}_8\text{F}_{17}\text{Br}$. The fact that k_{act} of PEBR was 3.5 times higher than that of $\text{C}_8\text{F}_{17}\text{Br}$ (experiment nos. 2 and 4 in Table 2) implies a better reactivity of the growing macromolecular chains $[\text{C}_8\text{F}_{17}-(\text{poly}(\text{styrene}))-\text{Br}]$ than that of the $\text{C}_8\text{F}_{17}\text{Br}$ initiator. This confirmation can partially explain the lack of control of the polymerization of styrene by ATRP. This is in agreement with the nonquantitative consumption of the initiator ($\text{C}_8\text{F}_{17}\text{Br}$) and the difference between the experimental and theoretical molecular weights.

Then, all ATRP polymerizations of styrene below using $\text{C}_8\text{F}_{17}\text{Br}$ as the initiator were performed at 110 °C with $\text{Cu}^{\text{I}}\text{Br}/\text{HMTETA}$ as the catalytic system in DMF.

Typical SEC curves for controlled radical polymerization are displayed in Figure 2. THF was used as the eluent while SEC apparatus was equipped with a refractive index detector. Hence,

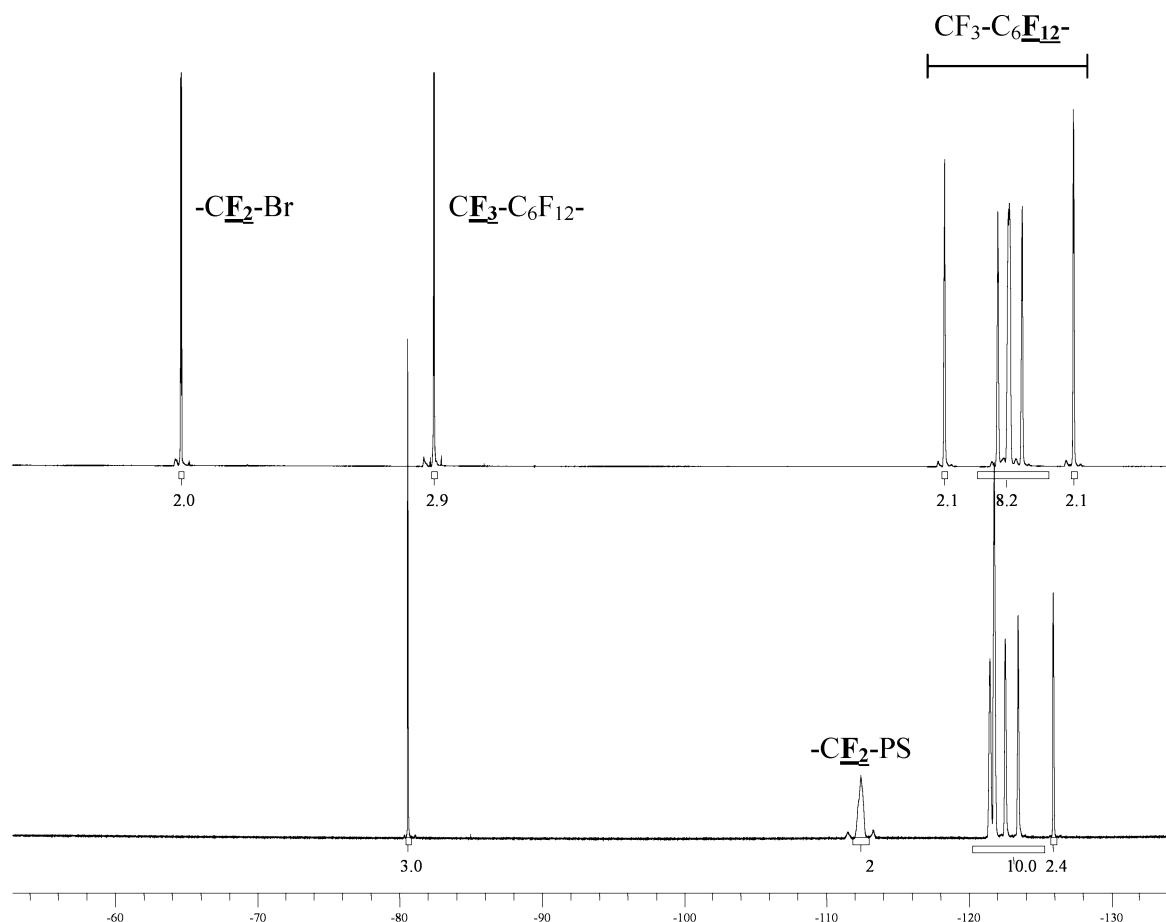


Figure 5. ^{19}F NMR spectra of $\text{C}_8\text{F}_{17}\text{Br}$ (upper figure) and C_8F_{17} -poly(styrene) (lower figure) synthesized by ATRP of styrene using $\text{C}_8\text{F}_{17}\text{Br}$ as the initiator (recorded in deuterated acetone) (experiment no. 3, Table 1). Experimental conditions: $[\text{C}_8\text{F}_{17}\text{Br}]_0:[\text{styrene}]:[\text{Cu}^{\text{I}}\text{Br}]:[\text{HMTETA}]_0 = 3.3:100.0:1.0:1.0$; copper bromide (28.6 mg, 2×10^{-4} mol), 1,1,4,7,10,10-hexamethyltriethylenetetramine (HMTETA) (46.6 mg, 2×10^{-4} mol), $\text{C}_8\text{F}_{17}\text{Br}$ (0.33 g, 6.67×10^{-4} mol) and styrene (2.08 g, 2×10^{-2} mol) and 10.0 g of DMF.

Table 2. Activation Rate Constants Measured in Acetonitrile at 35 °C^a

RX initiator	Structure	Catalytic System	k_{act} ($\text{M}^{-1}\cdot\text{s}^{-1}$) at 35 °C	Ref.
EBriB	$\begin{array}{c} \text{CH}_3 \\ \\ \text{CH}_3-\text{C}-\text{Br} \\ \\ \text{C}=\text{O} \\ \\ \text{OCH}_2\text{CH}_3 \end{array}$	$\text{Cu}^{\text{I}}\text{Br}/\text{PMDETA}$	1.700	48
PEBr	$\begin{array}{c} \text{CH}_3\text{CH}-\text{Br} \\ \\ \text{C}_6\text{H}_5 \end{array}$	$\text{Cu}^{\text{I}}\text{Br}/\text{PMDETA}$	0.120	48
MBrP	$\begin{array}{c} \text{H} \\ \\ \text{CH}_3-\text{C}-\text{Br} \\ \\ \text{C}=\text{O} \\ \\ \text{OCH}_3 \end{array}$	$\text{Cu}^{\text{I}}\text{Br}/\text{PMDETA}$	0.110	48
$\text{C}_8\text{F}_{17}\text{Br}$	$\text{R}_f\text{CF}_2-\text{Br}$	$\text{Cu}^{\text{I}}\text{Br}/\text{HMTETA}$	0.035	This work

^a Note: PMDETA and HMTETA stand for *N,N,N',N',N''*-pentamethyldiethylenetriamine and 1,1,4,7,10,10-hexamethyltriethylenetetramine.

hydrogenated and fluorinated compounds were detected as positive and negative signals, respectively. Consequently, the decrease of the negative signal arising from the consumption of $\text{C}_8\text{F}_{17}\text{Br}$ for the initiation of styrene. In addition, the curves shifting toward low retention times when monomer conversion was increasing indicate an increase of the molecular weights of the resulting grafted copolymers. The molecular weight

distributions or polydispersity indexes (PDI) are slightly larger for those corresponding to the polymers obtained from the ATRP of styrene but remained lower than those produced from conventional radical polymerizations. No evidence, such as multimodal SEC signals (suggesting thermal initiation of styrene) was noted for the reported polymers.⁴⁹ Interestingly, the polydispersity indexes slowly decreased throughout the polymerization, reaching a value of 1.78 for 70% of styrene conversion. Nevertheless, a tailing was observed with the increase of the molecular weight suggesting a lack of the control of the polymerization at high conversion rates.

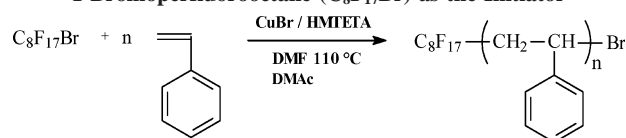
The kinetics plots of the polymerization are shown in Figure 3 (and in Figure 6 of the Supporting Information). That latter figure represents a $\ln([\text{styrene}]_0/[\text{styrene}])$ vs polymerization time linear relationship, where $[\text{styrene}]_0$ and $[\text{styrene}]$ stand for the styrene concentrations at $t = 0$ and at t time, respectively. The apparent polymerization rate was first order with respect to monomer concentration, which means that the concentrations of the growing radicals are constant. The apparent rate coefficients ($k_p^{\text{app}} = -d(\ln[M])/dt$) can be obtained from the slope of the straight line given by the kinetics plot. Deviation from linear kinetics occurs at long reaction times due to some side reactions including elimination and termination.⁵⁰ Both elimination and termination steps removed $\text{C}_8\text{F}_{17}\text{Br}$ from the reaction. In addition, termination also reduced $[\text{Cu}^{\text{I}}]$ concentration and increased $[\text{Cu}^{\text{II}}]$ concentration. The overall effect resulted in the decrease of the polymerization rate. Figure 3 represents the

Table 3. Determination of the Composition of Comonomers in the Poly(VDF-co-BDFO) Copolymers vs the Reaction Conditions in the Radical Copolymerization of Vinylidene Fluoride (VDF) with 8-Bromo-1*H*,1*H*,2*H*-perfluorooct-1-ene (BDFO) (Initiated by 2,5-Bis(*tert*-butylperoxy)-2,5-dimethylhexane (DHBP) at 134 °C for 7 h)

expt no.	VDF ^a in feed (mol %)	BDFO in feed (mol %)	C ₀ (%)	gaseous convn (%)	yields by mass (%)	VDF in copolymer (mol %)	BDFO in copolymer (mol %)	no. of BDFO by chain ^b	T _d (°C) ^c Δ <i>m</i> (5%)	T _g (°C)	M _n ^d	PDI ^d
7	95.5	4.5	1.1	85	75	96.4	3.6	6	340	-16	12 800	5.0
8	95.0	5.0	0.8	60	54	93.9	6.1	11	345	-16	15 000	2.3
9	90.8	9.2	1.2	56	50	87.8	12.2	12	325	-12	10 200	2.5

^a The content of different comonomers could be calculated as follows: mol % VDF in the copolymer = $I_A/(I_A + I_B) \times 100$, where $I_A = (I_{-43.2} + I_{-91.4} + I_{-94.8} + I_{-113.8} + I_{-116.0})/2$ and $I_B = I_{-64.9}/2$ where I_{-x} represents the integral of the signal centered at $-x$ ppm in the ^{19}F NMR spectrum of poly(VDF-co-BDFO) copolymers (see Table 1 in the Supporting Information). ^b Calculated from the equation: number of BDFO by chain = $[\text{BDFO}]_{\text{in copolymer}} \times M_n / [(\text{VDF})_{\text{in copolymer}} \times M^{\text{VDF}} + (\text{BDFO})_{\text{in copolymer}} \times M^{\text{BDFO}}]$, where M^{VDF} , M^{BDFO} and M_n , $[\text{VDF}]_{\text{in copolymer}}$, and $[\text{BDFO}]_{\text{in copolymer}}$ correspond to the molecular weights of VDF, BDFO and poly(VDF-co-BDFO) copolymers, to the composition in VDF of copolymer, and to the composition of BDFO in copolymer, respectively. ^c Thermal stability determined by TGA under air (5% loss). ^d Determined by SEC chromatography (using poly(styrene) standards).

Scheme 2. Atom Transfer Radical Polymerization (ATRP) of Styrene in the Presence of Cu^IBr/1,1,4,7,10,10-hexamethyltriethylenetetramine (HMTETA) as the Catalytic System, Dimethylformamide (DMF) or Dimethylacetamide (DMAc) as the Solvent, and 1-Bromoperfluorooctane (C₈F₁₇Br) as the Initiator



evolution of molecular weights vs the monomer conversion showing a linear dependence. However, the experimental molecular weights were higher than the theoretical ones, and this observation may arise from the low value of the activation rate constant of C₈F₁₇Br initiator.

Characterization of C₈F₁₇-Poly(styrene)s. The polymerization of styrene initiated by C₈F₁₇Br was also evidenced by NMR spectroscopy. Figure 4 shows a typical ^1H NMR spectrum of a poly(styrene) synthesized by using C₈F₁₇Br as the initiator. First, the presence of two characteristic signals of poly(styrene) is noted: (i) in the 6.5–7.4 ppm range assigned to the aryl protons of styrene units and (ii) in the 1.2–2.1 ppm range attributed to the methylene and methyne protons of the poly(styrene) backbone. Interestingly, additional signals located in the 4.2–4.7 ppm and in the 2.5–2.8 ppm ranges are assigned to $-\text{CH}(\text{C}_6\text{H}_5)\text{Br}$ and $\text{R}-\text{CF}_2-\text{CH}_2-\text{CH}(\text{C}_6\text{H}_5)-$ end groups, respectively. On the other hand, the ^{19}F NMR spectrum of a poly(styrene) synthesized using C₈F₁₇Br as the initiator (Figure 5) shows the absence of signal centered at -65 ppm assigned to $\text{C}_7\text{F}_{15}-\text{CF}_2-\text{Br}$ extremity, and evidences the ATRP process via C₈F₁₇Br initiator. This observation excludes the hypothesis of thermal polymerization of styrene and is in agreement with the study of Zhang et al.¹⁶ Figure 5 also exhibits the presence of an AB system located at -112.5 ppm attributed to the difluoromethylene group adjacent to the first styrenic unit. Finally, the signal assigned to the difluoromethylene group, located in the β position about the bromine atom for the C₈F₁₇Br initiator, centered at -118.5 ppm, underwent a high field shift to -121.5 ppm when the polymerization occurred.

An oligo(styrene) synthesized by ATRP ($M_n = 4300 \text{ g}\cdot\text{mol}^{-1}$ and PDI = 1.7, experiment no. 3, Table 1, determined by SEC with poly(styrene) standards) was also studied by matrix-assisted laser desorption-ionization time-of-flight mass spectrometry (MALDI-TOF-MS). The analyses were carried out in reflection mode using 2,3,4,5,6-pentafluorocinnamic acid (PFCA) as the matrix. Sodium iodide was added as the cationization agent. Consequently, a Na⁺ cation might be complexed with each macromolecule. Figure 6 represents the MALDI-TOF mass

spectrum of that analyzed R_F-oligo(styrene). The difference of mass between peaks was $104.06 \text{ g}\cdot\text{mol}^{-1}$, corresponding to one styrene unit. For example, the expansion of the zone $m/z = 3600\text{--}4000 \text{ g}\cdot\text{mol}^{-1}$ exhibits two different series: (i) first, the expected $\text{C}_8\text{F}_{17}-[\text{CH}_2-\text{CH}(\text{C}_6\text{H}_5)]_{32}-\text{Br}/\text{Na}^+$ is located at $m/z 3850 \text{ g}\cdot\text{mol}^{-1}$ (series A) with a strong intensity; (ii) second, a distribution at $3770 \text{ g}\cdot\text{mol}^{-1}$ (series B) with a weak intensity can be ascribed to the elimination of HBr in the polymeric chains of structure A. This loss of HBr induces a vinyl-terminated poly(styrene). It can occur either at a temperature higher than 150 °C or in the course of the MALDI-TOF analysis.^{51–53} Moreover, it is important to note the absence of the distribution corresponding to the thermal initiation of styrene, which would appear at $3767 \text{ g}\cdot\text{mol}^{-1}$ for $[\text{CH}_2-\text{CH}(\text{C}_6\text{H}_5)]_{36}/\text{Na}^+$. Thus, the MALDI-TOF analysis confirms that the polymers obtained from ATRP was initiated by C₈F₁₇Br, yielding original poly(styrene)s which bear the C₈F₁₇- end group. In addition, the C₈F₁₇ group does not disturb the MALDI-TOF analysis.

As the ATRP of styrene was successfully achieved from C₈F₁₇Br as the initiator, the experimental conditions of this model were extended to original copolymers based on VDF units and bearing perfluorobrominated side groups.

(2) Graft Polymerization of Styrene with Poly(VDF-co-BDFO) Copolymers via ATRP. The fluorinated poly(VDF-co-BDFO) copolymeric initiators bearing $-\text{CF}_2\text{Br}$ dangling groups were achieved by radical copolymerization of vinylidene fluoride (VDF) and 8-bromo-1*H*,1*H*,2*H*-perfluorooct-1-ene (BDFO), initiated by 2,5-bis(*tert*-butylperoxy)-2,5-dimethylhexane (DHBP), in 1,1,1,3,3-pentafluorobutane as the solvent, at 134 °C for 7 h³⁴ (Scheme 4).

The synthesis of BDFO, reported in the Supporting Information, was achieved in two steps: (i) by ethylenation of commercially available $\text{Br}-\text{C}_6\text{F}_{12}-\text{Br}$, (ii) followed by the dehydrobromination of the monoadduct in the presence of KOH in methanol. After work up and distillation, the monomer, characterized by ^1H , ^{19}F , and ^{13}C NMR spectroscopies (Figures 1–3 in the Supporting Information, respectively), was obtained in 79% yield.

Three radical copolymerizations of VDF and BDFO (Table 3) were carried out using an initial $[\text{initiator}]_0/([\text{VDF}]_0 + [\text{BDFO}]_0)$ molar ratio (C_0) ranging from 0.8 to 1.2 mol % and $[\text{VDF}]_0/[\text{BDFO}]_0$ initial molar ratios (in feed) of 90/10 and 95/5, respectively. The initial amounts of BDFO were chosen low (from 5 to 15% in feed) compared to that of VDF since a few amount of BDFO in the copolymer was necessary to enable further initiation of styrene by ATRP via the brominated $-\text{CF}_2\text{Br}$ end group. The number of $-\text{CF}_2\text{Br}$ moieties by chain ranged from 6 to 12 (number of BDFO

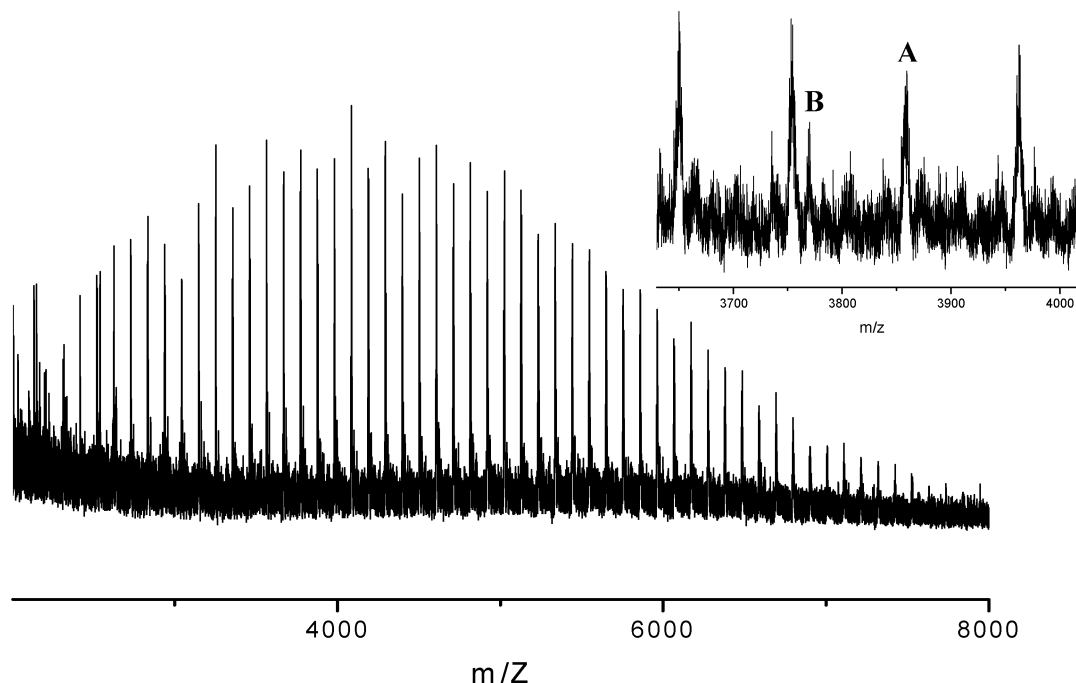
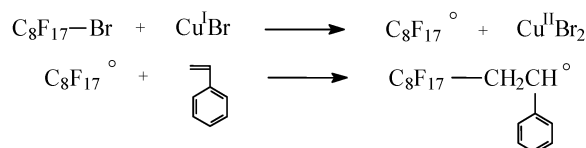


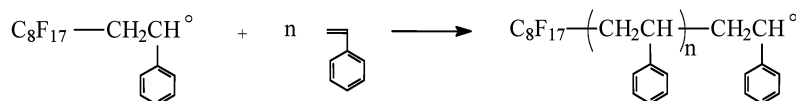
Figure 6. MALDI-TOF mass spectrum of C_8F_{17} -poly(styrene) synthesized by ATRP using $C_8F_{17}Br$ as the initiator ($M_n = 4300 \text{ g mol}^{-1}$ and $PDI = 1.7$ (experiment no. 3, Table 1) assessed by size exclusion chromatography with poly(styrene) standards) in 2,3,4,5,6-pentafluorocinnamic acid (PFCA) as the matrix. These C_8F_{17} -poly(styrene)s were Na^+ cationized (addition of NaI in the polymeric solution). The data were acquired in a reflectron mode. Experimental conditions: $[C_8F_{17}Br]_0:[styrene]:[Cu^I Br]_0:[HMTETA]_0 = 3.3:100.0:1.0:1.0$; copper bromide (28.6 mg, 2×10^{-4} mol), 1,1,4,7,10,10-hexamethyltriethylenetetramine (HMTETA) (46.6 mg, 2×10^{-4} mol), $C_8F_{17}Br$ (0.33 g, 7×10^{-4} mol), and styrene (2.08 g, 2×10^{-2} mol) and 10.0 g of DMF, experiment no. 3, Table 1.

Scheme 3. Main Steps in the Atom Transfer Radical Polymerization (ATRP) of Styrene Initiated by 1-Bromoperfluorooctane ($C_8F_{17}Br$)^a

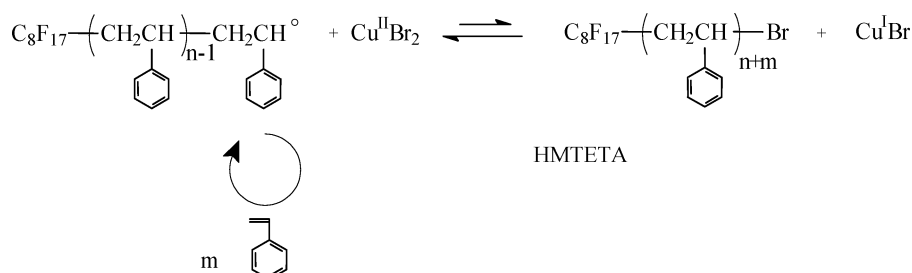
Initiation :



Propagation :

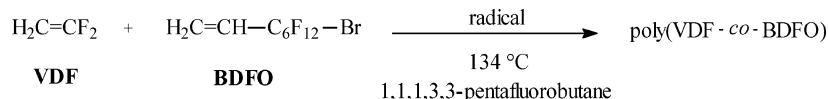


Reversible termination :



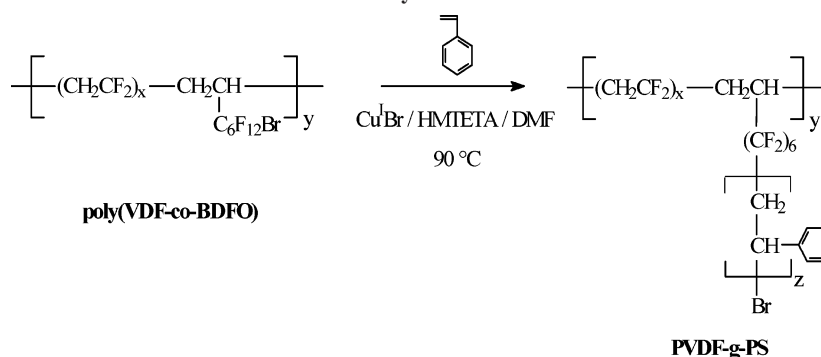
^a HMTETA stands for 1,1,4,7,10,10-hexamethyltriethylenetetramine.

Scheme 4. Radical Copolymerization of Vinylidene Fluoride (VDF) with 8-Bromo-1*H*,1*H*,2*H*-perfluorooct-1-ene (BDFO)



by chain = $[BDFO^{\text{in copolymer}} \times M_n]/[(VDF^{\text{in copolymer}} \times M^{\text{VDF}}) + (BDFO^{\text{in copolymer}} \times M^{\text{BDFO}})]$, where M^{VDF} , M^{BDFO} , M_n , $VDF^{\text{in copolymer}}$ and $BDFO^{\text{in copolymer}}$ correspond to the molecular

weights of VDF, BDFO and poly(VDF-co-BDFO) copolymers and to the compositions of VDF and BDFO in the copolymers, respectively). After reaction, the copolymers were precipitated

Scheme 5. Synthesis of Poly(vinylidene fluoride)-g-poly(styrene) Graft Copolymers by Atom Transfer Radical Polymerization of Styrene^a

^a Note: VDF, BDFO, HMTETA, and DMF stand for vinylidene fluoride, 8-bromo-1H,1H,2H-perfluorooct-1-ene, 1,1,4,7,10,10-hexamethyltriethylenetetramine, and dimethylformamide, respectively.

Table 4. Experimental Conditions of ATRP of Styrene Initiated by Poly(VDF-co-BDFO) Copolymer

experiments	initial concentrations [DMF] ₀ : [styrene] ₀ : [Br] ₀ : [HMTETA] ₀ : [Cu ^I Br] ₀	temp (°C)	observations
10	100.0:100.0:1.0:1.0:1.0	110	cross-linking
11	100.0:100.0:1.0:1.0:1.0	90	styrene conversion of 6–8% followed by cross-linking
12	100.0:100.0:1.0:0.5:0.5	110	styrene conversion of 15% followed by cross-linking
13	100.0:100.0:1.0:0.5:0.5	90	styrene conversion of 20% followed by cross-linking
14a	500.0:100.0:1.0:0.0:0.0	90	low conversion of styrene (5%)
14b	500.0:100.0:1.0:0.5:0.5	90	polymerization, styrene conversion 60–70%

DMF and HMTETA stand for dimethylformamide and 1,1,4,7,10,10-hexamethyltriethylenetetramine, respectively.

Table 5. Graft Copolymerization of Styrene Initiated by Poly(VDF-co-BDFO) Copolymers at 90 °C (Poly(VDF-co-BDFO) Copolymers 8 in Table 3)^f

expt no.	poly(VDF-co-BDFO) copolymer	solvent	[Br] ₀ : [styrene] ₀ : [Cu ^I Br] ₀ : [HMTETA] ₀ ^a	targeted M_n (g mol ⁻¹)	α^b (%)	theor M_n^c (g mol ⁻¹)	exptl M_n^d (g mol ⁻¹)	PDI ^d	graft M_n^e (g mol ⁻¹)
15a	8	DMF	1.0:100.0:0.0:0.0	—	—	—	15 000	2.3	0
15b	8	DMF	1.0:100.0:0.5:0.5	125 000	70	92 000	90 800	2.2	8100
16	8	DMF	5.0:100.0:0.5:0.5	37 500	70	30 000	28 300	2.5	1400
17	8	DMF	2.5:100.0:0.5:0.5	72 000	85	60 000	59 000	2.7	4000
18	8	DMF	1.0:100.0:0.5:0.5	130 800	70	91 000	78 000	2.6	6800

^a [Br]₀: [styrene]₀: [Cu^IBr]₀: [HMTETA]₀ is the initial molar ratio of bromine atom (macronitiator), monomer, CuBr, and ligand, respectively. ^b Styrene conversion determined by gas chromatography and by ¹H NMR. ^c Targeted molecular weights determined by: $M_n = n_{Br} (\alpha \times [\text{styrene}]_0) / [\text{Br}]_0 + M_{n \text{ poly(VDF-g-BDFO)}}$, where α , [styrene]₀, [Br]₀, $M_{n \text{ poly(VDF-g-BDFO)}}$, and n_{Br} represent the styrene conversion, the concentrations of styrene and of bromine of poly(VDF-co-BDFO), the molecular weight of poly(VDF-g-BDFO) copolymers, and the number of bromine per chain, respectively. ^d Molecular weights and polydispersity indexes determined by size exclusion chromatography (using styrene standards and UV detector). ^e Graft molecular weight calculated by the equation $M_n = (M_{n \text{ copolymer}} - M_{n \text{ initial}}) / \text{number of Br atom by chain}$, with $M_{n \text{ copolymer}}$ determined by SEC after grafting of styrene, $M_{n \text{ initial}}$ corresponding to the molecular weight of poly(VDF-co-BDFO) copolymers before grafting of styrene. The molecular weights of the graft copolymers obtained by SEC calibrated by linear poly(styrene) standards are apparent. ^f Note: DMF and HMTETA stand for dimethylformamide and 1,1,4,7,10,10-hexamethyltriethylenetetramine, respectively (eq 1).

from cold pentane twice and, after drying, the products (soluble in acetone) were characterized by ¹H and ¹⁹F NMR spectroscopies.

Figure 4 in the Supporting Information represents the ¹⁹F NMR spectrum of a poly(VDF-co-BDFO) copolymer from a feed content of VDF/BDFO molar ratio of 95.0/5.0. First, it shows the characteristic signal centered at -91.4 ppm (-CH₂-CF₂-CH₂-) resulting from the head-to-tail addition of VDF. Moreover, a series of other signals, also assigned to difluoromethylene of VDF, located at -94.8, -113.8 and -116.0 ppm attributed to difluoromethylene groups in -(CH₂-CF₂)-(CF₂-CH₂)-(CH₂-CF₂)-(CH₂-), -(CH₂-CF₂)-(CF₂-CH₂)-(CH₂-) and -(CH₂-CF₂)-(CF₂-CH₂)-(CH₂-CF₂-),^{54–60} respectively (Table 1 in the Supporting Information). These three last signals resulted from the inversion of VDF unit in the chain (head-to-head addition). Furthermore, the signal centered at -94.8 ppm is assigned to the difluoromethylene group of the VDF unit adjacent to a BDFO unit. That located at -43.2 ppm

is assigned to -(CH₂-CF₂)-[CH₂-CH(C₆F₁₂-CH₂-CF₂-Br)]- resulting from an insertion of VDF after homolytic cleavage of the C-Br bond of BDFO under radicals^{61,62} (see Figure 4 in the Supporting Information). It is remarkable to note the great low field shift of the signal centered at -64.9 ppm (assigned to -CF₂-CF₂-Br) to -43.2 ppm (assigned to -CH₂-CF₂-Br) that confirms previous works.^{61,62} However, as mentioned below, the amount of transfer is low (3%). As expected, difluoromethylene side-group adjacent to CH in the backbone leads to an AB system since both fluorine atoms are anisochronous ($\delta_1 = -116.5$ ppm and $\delta_2 = -120.0$ ppm), with a slight overlapping with the signals centered in the -117.1 to -123.1 ppm range attributed to the characteristic difluoromethylene groups in the pendant chain of BDFO units. Finally, the signal located at -64.9 ppm is assigned to the difluoromethylene group adjacent to the bromine atom in BDFO (Table 1 and Figure 4 in the Supporting Information).

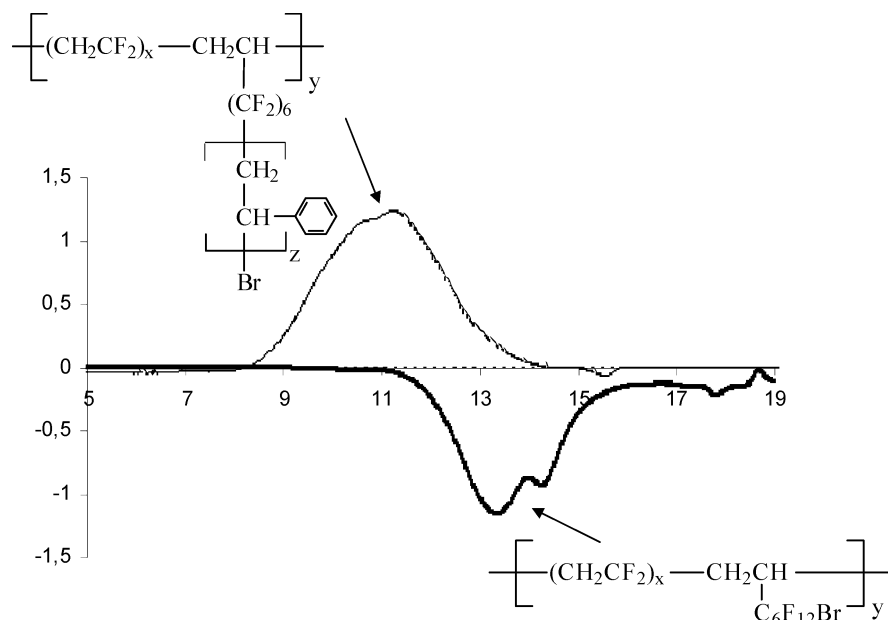


Figure 7. Evolution of size exclusion chromatography (SEC) traces of poly(VDF-*co*-BDFO) (negative signal) and PVDF-*g*-PS (positive signal) copolymers after ATRP of styrene using poly(VDF-*co*-BDFO) copolymer as the macroinitiator. $[\text{Br}]_0:[\text{styrene}]_0:[\text{HMTETA}]_0:[\text{Cu}^{\text{I}}\text{Br}]_0 = 1.0:100.0:0.5:0.5$; $T = 90^\circ\text{C}$, experiment no. 18 in Table 5. DMF and HMTETA stand for dimethylformamide and 1,1,4,7,10,10-hexamethyltriethylenetetramine, respectively.

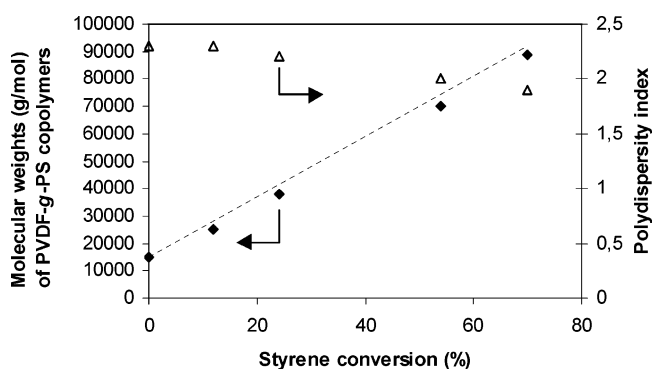


Figure 8. Dependence of molecular weights (\blacklozenge) and polydispersity indexes (Δ) of PVDF-*g*-PS copolymers vs styrene conversion for the atom transfer radical polymerization (ATRP) of styrene using poly(VDF-*co*-BDFO) copolymers as the macroinitiators. $[\text{Br}]_0:[\text{styrene}]_0:[\text{HMTETA}]_0:[\text{Cu}^{\text{I}}\text{Br}]_0 = 1.0:100.0:0.5:0.5$; $T = 90^\circ\text{C}$ (experiment no. 18 Table 5). VDF, BDFO, HMTETA, and DMF stand for vinylidene fluoride, 8-bromo-1*H*,1*H*,2*H*-perfluorooct-1-ene, 1,1,4,7,10,10-hexamethyltriethylenetetramine, and dimethylformamide, respectively. The dotted straight line represents the theoretical curve. Note: The molecular weights of graft copolymers obtained from SEC calibrated are apparent values, which are smaller than the absolute molecular weights.

By comparison with the integrals of the multiplets located at -43.2 ppm, in the -90.0 to -95.0 ppm and -113.8 to -116.0 ppm range (assigned to the difluoromethylene group of VDF) with the signal centered at -64.9 ppm (attributed to $-\text{CF}_2\text{Br}$ in BDFO), the content of different comonomers can be assessed (Table 3) as follows (eq 4):

$$\text{mol \% of VDF in the copolymer} = \frac{I_A}{I_A + I_B} \times 100 \quad (4)$$

$$\text{with } I_A = (I_{-43.2} + I_{-91.4} + I_{-94.8} + I_{-113.8} + I_{-116.0})/2 \text{ and } I_B = I_{-64.9}/2$$

The results are listed in Table 3. Indeed, the ^{19}F NMR characterization of their microstructures evidenced that random copolymers were obtained in which microblocks of PVDF were separated by one BDFO unit. This observation confirms that

BDFO is not able to homopolymerize, and the same behavior was observed for the radical copolymerization of VDF with perfluoroalkylvinyl ether,^{63,64} trifluorovinylaryloxy monomers,^{65,66} 2-pentafluorosulfanyl-1,1,2-trifluoroethene,⁶⁷ or HFP.⁶⁸ Nevertheless, according to Table 3, it is clearly observed that BDFO is active enough to be incorporated in sufficient amount into the poly(VDF-*co*-BDFO) copolymers. In addition, three statements can be deduced from these first results.

1. The radical copolymerization of both comonomers was successfully achieved (Yield > 50%) when the molar ratio of BDFO in feed was lower than 10%, as evidenced by the presence of the characteristic ^{19}F and ^1H NMR signals of the expected groups attributed to both monomers.
2. The fluorinated side chain keeps its bromine end atom ($-\text{CF}_2-\text{Br}$) in the course of the copolymerization.
3. By comparison between the integrals of the triplet of triplets located at -43.2 ppm (assigned to $-\text{CF}_2-\text{CH}_2-\text{CF}_2-\text{Br}$) with that of the triplet centered at -64.9 ppm (attributed to the $\text{R}_f-\text{CF}_2-\text{Br}$ of BDFO), the percentage of transfer to the $-\text{R}_f-\text{Br}$ side chain of BDFO comonomer was assessed by eq 5:

$$\% \text{ of transfer to BDFO} = \frac{I_{-43.2}}{I_{-43.2} + I_{-64.9}} \times 100 = 3\% \quad (5)$$

The ^1H NMR spectrum (Figure 5 in the Supporting Information) exhibits the presences of the characteristic multiplets centered at 2.9 and 2.3 ppm assigned to the methylene groups in $-\text{CH}_2-\text{CF}_2-\text{CH}_2-\text{CF}_2-\text{CH}_2-\text{CF}_2-$ and $-\text{CF}_2-\text{CH}_2-\text{CH}_2-\text{CF}_2-$ sequences resulting from the normal tail-to-head and reversed tail-to-tail VDF additions. Furthermore, the ^1H NMR spectra show a triplet located at 1.0 ppm ($^3J_{\text{HH}} = 7.5$ Hz) generally attributed to $-\text{CF}_2-\text{CH}_2-\text{CH}_3$.^{58,59} This end group could result from the direct initiation of CH_3° onto VDF, arising from the decomposition (at 134°C) of DHBP initiator which undergoes a thermal decomposition by homolytic cleavage of the O–O bonds, hence generating tBuO° radicals which produce CH_3° and acetone after rearrangement.^{58,62}

The results of the copolymerization (experimental conditions and feed vs contents of comonomers in the copolymers) are

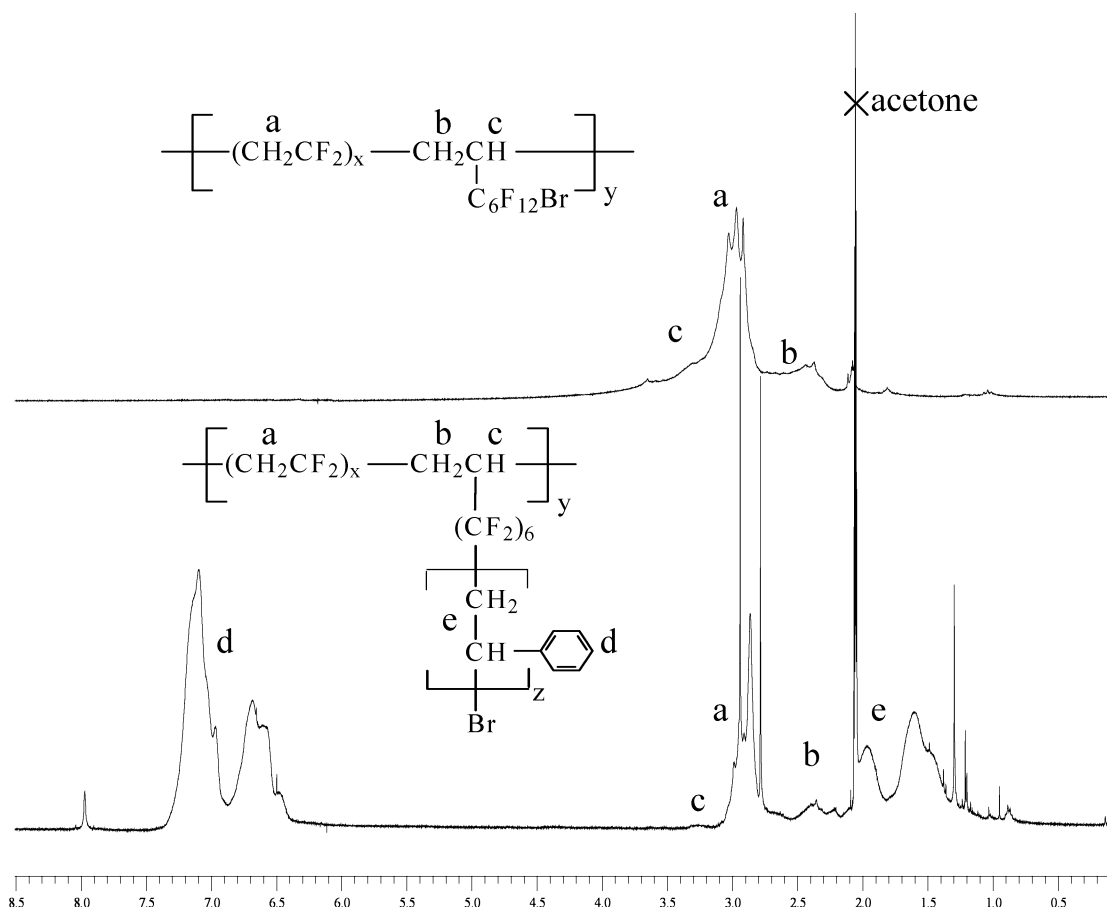


Figure 9. ^1H NMR spectra of poly(VDF-*co*-BDFO) copolymer (upper figure) and PVDF-*g*-PS graft copolymer (lower figure) (recorded in deuterated acetone). $[\text{Br}]_0:[\text{styrene}]_0:[\text{HMTETA}]_0:[\text{Cu}^+\text{Br}]_0 = 1.0:100.0:0.5:0.5$; $T = 90^\circ\text{C}$ (experiment no. 18 Table 5). VDF, BDFO, and HMTETA stand for vinylidene fluoride, 8-bromo-1*H*,1*H*,2*H*-perfluorooct-1-ene, and 1,1,4,7,10,10-hexamethyltriethylenetetramine, respectively. The resonances located at 2.75, 2.92, and 7.95 ppm are assigned to the chemical shifts of dimethylformamide.

summarized in Table 3. PVDF-*g*-PS graft copolymers were synthesized by ATRP of styrene in the presence of these poly(VDF-*co*-BDFO) statistic copolymers (Scheme 5).

ATRP reactions were carried out in DMF. Actually, fluoropolymers such as PVDF exhibit poor solubility in solvents commonly involved in ATRP process. This is the case for DMF while it is a suitable solvent of poly(VDF-*co*-BDFO) macroinitiator. In fact, preliminary tests of radical polymerization of styrene using poly(VDF-*co*-BDFO) copolymer as the macroinitiator in the presence of Cu^+Br and HMTETA led to cross-linking. The coupling of radicals of the side groups during the polymerization induced the formation of a network. This observation is in agreement with the results obtained by Zhang and Russell.³³ On the other hand, this side reaction is also well-known to synthesize telechelic compounds.^{69,70} Indeed, the constants of these terminations (such as the coupling reaction) are proportional to $k_t[\text{P}^\bullet]^2$. Various different parameters of ATRP of styrene in the presence of the poly(VDF-*co*-BDFO) copolymers have been studied: the amount of ligand, the amount of catalytic system ($\text{CuBr}/\text{HMTETA}$, $\text{CuBr}/\text{bipyridine}$), the reaction temperature (ranging from 90 to 110 $^\circ\text{C}$) and the concentration to reduce the amount of radicals in the medium. Tables 4 and 5 summarize the initial conditions (reactant feed ratios, concentrations, and experimental conditions) to avoid any coupling reaction and to improve the styrene conversion.

The evidence of that atom transfer radical polymerization was provided by monitoring the evolution of the molecular weights of the resulting PVDF-*g*-PS graft copolymers by SEC (Figure 7).

The curve shifting to the left when the monomer conversion was increasing indicates the evolution toward higher molecular weights. As above, SEC chromatograms (Figure 7) showed that the negative signal (from a refractive index detector) of the macroinitiator (arising from the presence of fluorinated segments) changed into a positive one corresponding to the increase of hydrogenated polystyrene grafts with respect to the fluorinated backbone. This is in agreement with a behavior noted for the syntheses of PVDF-*g*-PS graft³³ and PVDF-*b*-PS block^{18,20} copolymers. The absence of negative signal characteristic of the poly(VDF-*co*-BDFO) macroinitiator in the ATRP of styrene clearly demonstrates the grafting of styrene onto poly(VDF-*co*-BDFO) copolymers. Moreover, the absence of a polymeric network exhibits that there is no coupling reaction between $R_F\text{--Br}$ pendant groups, and this confirms the efficiency of initial conditions of ATRP.

Figure 7 in the Supporting Information plots the $\ln([\text{styrene}]_0/[\text{styrene}])$ vs time dependence. That linear relationship indicates that the polymerization is of first-order with respect to monomer and that the concentration of active species is constant throughout the reaction. The slope of the straight line enabled the assessment of the "apparent" rate constant, k_{app} , which worths $0.0050 \text{ L mol}^{-1} \text{ s}^{-1}$ at 90 $^\circ\text{C}$ in DMF.

Figure 8 represents the plots of the molecular weights (from SEC analysis) and the polydispersity indexes of PVDF-*g*-PS graft copolymers vs the styrene conversion. Interestingly, M_n increases with styrene conversion while polydispersity index slightly decreases (from 2.3 attributed to the statistical macroinitiator to 1.8 for that of the PVDF-*g*-PS graft copolymer) in

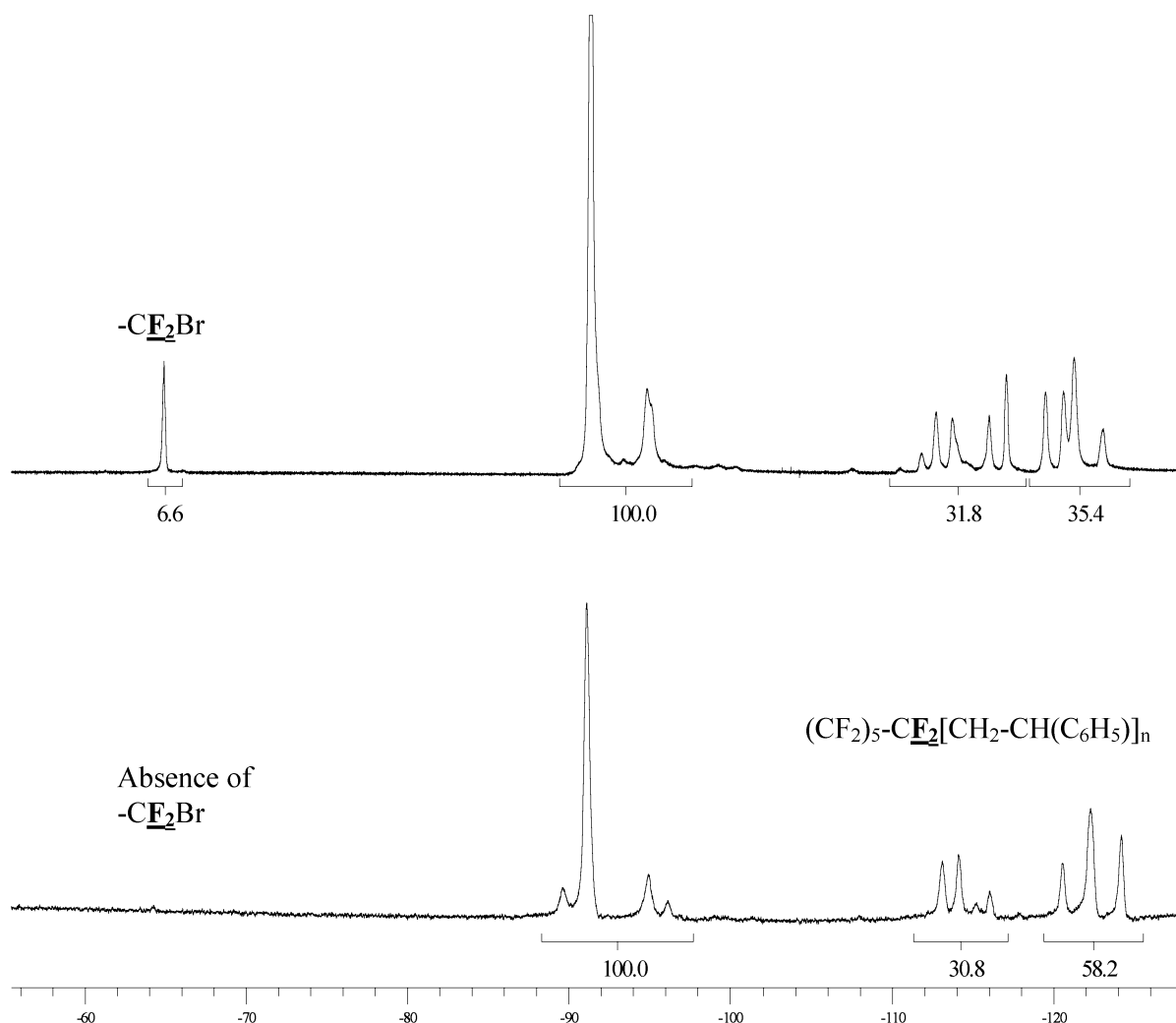


Figure 10. ^{19}F NMR spectra of poly(VDF-*co*-BDFO) copolymer (upper figure) and PVDF-*g*-PS graft copolymer (lower figure) (recorded in deuterated acetone). (Feed VDF/BDFO = 95/5 molar ratio; in the copolymer 93.9/6.1) $[\text{Br}]_0$: $[\text{styrene}]_0$: $[\text{HMTETA}]_0$: $[\text{Cu}^{\text{I}}\text{Br}]_0 = 1.0$:100.0:0.5:0.5; $T = 90^\circ\text{C}$ (experiment no. 18, Table 5). VDF, BDFO, and HMTETA stand for vinylidene fluoride, 8-bromo-1*H*,1*H*,2*H*-perfluorooct-1-ene, and 1,1,4,7,10,10-hexamethyltriethylenetetramine, respectively.

the course of the radical graft polymerization as a first evidence of the controlled character. Moreover, the theoretical (dotted straight line in Figure 8) and the experimental values are in good agreement, and such a behavior confirms the controlled character of the radical polymerization. The molecular weights of the graft copolymers are apparent molecular weights, because the SEC apparatus was calibrated with linear poly(styrene) standards. Indeed, the molecular weights of the graft copolymers are smaller than the “absolute” molecular weights because of the compact structure probably linked to their different gyration radius compared to these of linear PS.

The graft molecular weights calculated by the equation:

$$\text{graft } M_n = \frac{(M_n^{\text{copolymer}} - M_n^{\text{initial}})/\text{number of Br atom per chain,}}{}$$

with $M_n^{\text{copolymer}}$ determined by SEC after grafting of styrene, M_n^{initial} correspond to molecular weight of poly(VDF-*co*-BDFO) before grafting of styrene.

The theoretical curve was determined from the equation

$$M_{n^{\text{theoretical}}} = [\text{styrene}]_0 \times \alpha_{\text{styrene}}/[\text{Br}]_0,$$

where $[\text{styrene}]_0$, $[\text{Br}]_0$, and α_{styrene} stand for the styrene and

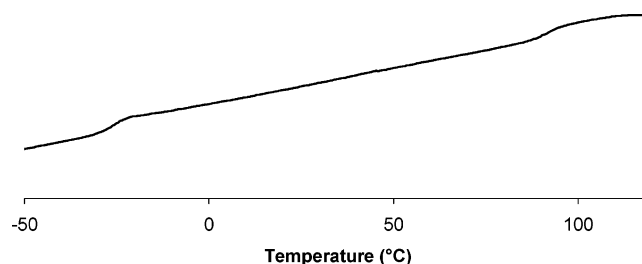


Figure 11. DSC thermogram of PVDF-*g*-PS graft copolymer (experiment no. 18 in Table 5).

bromine concentrations at initial time and styrene conversion, respectively.

Characterization of PVDF-*g*-PS Graft Copolymers. The satisfactory reactivity of styrene was also evidenced by NMR spectroscopy. Figure 9 exhibits typical ^1H NMR spectra of a poly(VDF-*co*-BDFO) macroinitiator and a PVDF-*g*-PS graft copolymer. The characteristic signals centered at 3.0 and 2.5 ppm are attributed to the head-to-tail and tail-to-tail addition of VDF units of the macroinitiator (Figure 8 in the Supporting Information), respectively. The spectrum of the PVDF-*g*-PS graft copolymer exhibits additional signals located in the 6.4–7.4 ppm and 1.5–2.1 ppm ranges assigned to the aromatic protons and to methylene and methyne groups of poly(styrene), respectively. In addition, the ^1H NMR spectrum confirms the absence

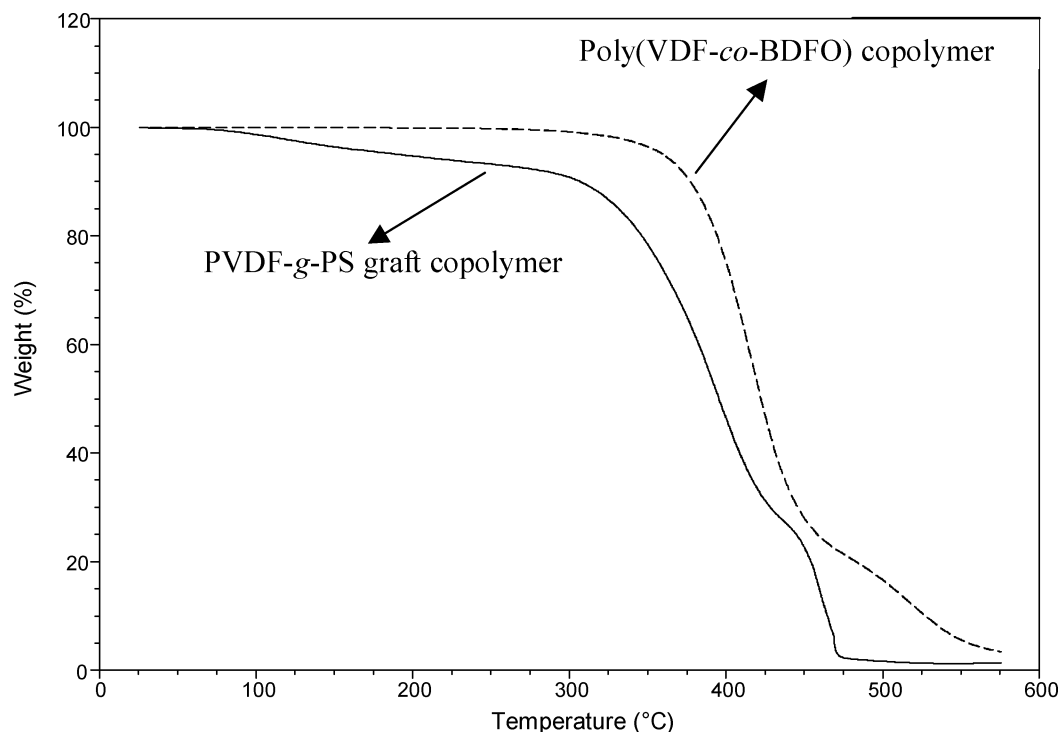


Figure 12. TGA thermograms of poly(VDF-*co*-BDFO) copolymer (dotted line, experiment no. 8 in Table 3) and PVDF-*g*-PS graft copolymers (full line, experiment no. 18 in Table 5) recorded under air.

of any signal in the 5.0–6.0 ppm range arising from possible dehydrofluorination of the VDF–BDFO diads (the possible basicity of HMTETA might decompose VDF units, via hydrofluoric acid elimination). Furthermore, the absence of the characteristic triplet of triplets centered at 6.15 ppm, assigned to $-\text{CF}_2\text{CF}_2\text{H}$ clearly indicates that no transfer reaction to the solvent, to the monomer or to the polymer occurred onto $-\text{C}_5\text{F}_{10}-\text{CF}_2^\bullet$ side radicals.

The characterization of the microstructure of PVDF-*g*-PS graft copolymers was also confirmed by ^{19}F NMR spectroscopy. Figure 10 represents the ^{19}F NMR spectra of a poly(VDF-*co*-BDFO) macroinitiator and of PVDF-*g*-PS graft copolymer. The latter figure shows the absence of the signal located at -65.0 ppm assigned to the $-\text{R}_f-\text{Br}$ extremity, and evidences its good reactivity as a quantitative consumption of $-\text{R}_f-\text{Br}$ units. As above, this spectrum shows the absence of both (i) the signals at about -100 ppm confirming the absence of any dehydrofluorination of the VDF–BDFO diads which could occur in the course of the ATRP reaction and (ii) that at about -136.0 ppm assigned to $-\text{CF}_2\text{H}$ end group in the $\text{C}_6\text{F}_{12}\text{H}$ dangling group, which also evidences the absence of the transfer to the monomer, to the solvent, or to the polymer. The simplification of complex signals assigned to the $-(\text{CF}_2)_4-\text{CF}_2\text{Br}$ of BDFO in the -120.0 to -125.0 ppm range is observed, this behavior arising from a certain symmetry of the perfluorinated chain also noted in VDF telomers.⁷¹

Thermal Properties of PVDF-*g*-PS Graft Copolymers. The glass transition temperatures (T_g) of PVDF-*g*-PS graft copolymers were assessed by differential scanning calorimetry (DSC). As expected, the thermograms exhibit two glass transition temperatures assigned to both blocks (Figure 11). The T_g values of poly(VDF-*co*-BDFO) copolymers incorporating 5–10 mol % of BDFO were ranging from -16 to -11 °C, respectively, hence being higher than that of PVDF ($T_g = -40$ °C) because of the presence of the $-\text{C}_6\text{F}_{12}\text{Br}$ grafts. After grafting poly(styrene), the resulting graft copolymers exhibit two T_g s at about -30 and $+90$ °C. The first one corresponds to the PVDF

backbone and it is obviously higher than that of PVDF because of the presence of poly(styrene) grafts. The second T_g depends on the molecular weight values, it is not surprising that the PS side segments exhibit a T_g ranging from 80 to 100 °C since their molecular weights are lower than $10\,000\text{ g mol}^{-1}$. For example, the molecular weights of poly(styrene) grafts in the analyzed graft copolymers were estimated at around 8100 g mol^{-1} and this explains such low T_g value.

The thermal stability of poly(VDF-*co*-BDFO) copolymers (Figure 9 of the Supporting Information) and of PVDF-*g*-PS graft copolymers were obtained by thermogravimetric analyses (TGA) (Figure 12). The thermograms of poly(VDF-*co*-BDFO) copolymers show a satisfactory thermal stability since the main decomposition, assigned to the dehydrofluorination of VDF–BDFO diads, occurs from 350 °C (5% in weight loss under air), while a second thermal degradation is noted from 450 to 490 °C characteristic of the PVDF backbone degradation. As expected, the thermograms of PVDF-*g*-PS graft copolymers show a lower thermostability than that of poly(VDF-*co*-BDFO) macroinitiator arising from the low molecular weight of the poly(styrene) grafts (of estimated molecular weights ca. 8100 g mol^{-1}). Thus, their TGA thermograms exhibit high weight losses in the 200–250 °C temperature range, as noted for PVDF-*b*-PS block copolymers²⁰ showing a superior thermal stability for PVDF polymeric main chain or block.

Conclusion

For the first time, 1-bromoperfluorooctane was successfully used as the initiator in the atom transfer radical polymerization (ATRP) of styrene. The activation rate constant of $\text{C}_8\text{F}_{17}\text{Br}$ ($k_{\text{act}} = 35 \times 10^{-3}\text{ M}^{-1}\text{ s}^{-1}$ at 35 °C in acetonitrile) was assessed and compared to those of the most widely used initiators in ATRP. The results show a better reactivity of the macromolecular chains in growth than the $\text{C}_8\text{F}_{17}\text{Br}$ initiator and explain the difference between experimental and theoretical molecular weights. Nevertheless, the ATRP process of styrene was

confirmed from kinetics data, NMR spectroscopy and SEC. Then, original macroinitiators comprising poly(vinylidene fluoride-co-8-bromo-1*H*,1*H*,2*H*-perfluorooct-1-ene), poly(VDF-co-BDFO) copolymers, prepared by radical copolymerization, initiated the ATRP of styrene successfully. Interestingly, the linear dependences of both the evolutions of $\ln([\text{styrene}]_0/[\text{styrene}])$ vs time and of the molecular weights of the resulting PVDF-g-PS graft copolymers vs the conversions of styrene, combined with the decrease of their polydispersity indexes vs the styrene conversion, evidenced the controlled behavior of that original “grafting from” radical copolymerization. The methodology of producing brominated poly(vinylidene fluoride) copolymers may prove a useful strategy of the general synthesis of macroinitiators for subsequent preparations of novel fluorinated graft copolymers. These obtained novel polymers may find potential applications as compatibilizers, surfactants, thin films, or emulsifiers for polymer blends between immiscible PVDF and PS homopolymers, under investigation.

Acknowledgment. The authors thank the European Community (program no. ENK-5-2002-00669 “Portapower”) and the Centre National de la Recherche Scientifique (CNRS) for financial support, Solvay S.A. compagne (Tavaux in France and Brussels in Belgium) for the gifts of vinylidene fluoride, and 1,1,1,3,3-pentafluorobutane, Atofina for the gift of 1-bromop-erfluorooctane and Gilles Valette (Université de Montpellier II) for MALDI-TOF MS spectroscopy.

Supporting Information Available: Text detailing the (i) synthesis and NMR characterization of 8-bromo-1*H*,1*H*,2*H*-perfluorooct-1-ene (BDFO), including a scheme presenting the synthesis and figures showing ^1H , ^{19}F , and ^{13}C NMR spectra, (ii) synthesis and characterization of copolymers obtained by radical copolymerization of VDF with BDFO, including ^{19}F and ^1H NMR spectra and a table of assignments of ^{19}F NMR shifts, and (iii) radical grafting of styrene onto poly(VDF-co-BDFO) copolymers, including figures showing a first-order plot of ATRP data, ^1H NMR spectra, and TGA thermograms. This material is available free of charge via the Internet at <http://pubs.acs.org>.

References and Notes

- Rempp, P. F.; Lutz, P. J. Synthesis of graft copolymers. In *Comprehensive Polymer Science*; Allen, G., Bevington, J. C., Eastmond, A. L., Russo, S., Eds.; Pergamon Press: Oxford, U.K., 1989; Vol. 6, Chapter 12, pp 403–421.
- Cowie, J. M. G. Block and Graft Copolymers. In *Comprehensive Polymer Science*; Allen, G., Bevington, J. C., Eastmond, A. L., Russo, S., Eds.; Pergamon Press: Oxford, U.K., 1989; Vol. 3(3) p 33.
- Borner, H. G.; Matyjaszewski, K. *Macromol. Symp.* **2002**, *177*, 1–15.
- Ameduri, B.; Boutevin, B. *Well-Architected Fluoropolymers: Synthesis, Properties and Applications*; Elsevier: Amsterdam, 2004.
- Seiler, D. A. PVDF in the chemical process industry. In *Modern Fluoropolymers*; Scheirs, J., Ed.; Wiley: New York, 1997; Chapter 25, p 487–505.
- Tai, H.; Wang, W.; Martin, R.; Liu, J.; Lester, E.; Licence, P.; Woods, H. M.; Howdle, S. M. *Macromolecules* **2005**, *38*, 355–363.
- Liu, Y.; Lee, J. Y.; Kang, E. T.; Wang, P.; Tan, K. L. *React. Funct. Polym.* **2001**, *47*, 201–213.
- Wang, P.; Tan, K. L.; Kang, E. T.; Neoh, K. G. *J. Mater. Chem.* **2001**, *11*, 783–789.
- Holmberg, S.; Holmlund, P.; Wilen, C.-E.; Kallio, T.; Sundholm, G.; Sundholm, F. *J. Polym. Sci., Part A: Polym. Chem.* **2002**, *40*, 591–600.
- Sun, W.; Chen, Y.; Zhou, L.; He, X. *J. Appl. Polym. Sci.* **2006**, *101*, 857–862.
- Boutevin, B.; Robin, J. J.; Serdani, A. *Eur. Polym. J.* **1992**, *28*, 1507–1511.
- Kawashima, C.; Yasumura, T. (Central Glass Co., Ltd., Japan). US, 4,472,557, 1984.
- Davis, K. A.; Matyjaszewski, K. *Adv. Polym. Sci.* **2002**, *159*, 2–166.
- Yutani, Y.; Tatamoto, M. (Daikin): EP, 0489370 A1, 1991.
- Carlson, D. P. (Dupont de Nemours and Co.): US, 5,284,920, 1994.
- Zhang, Z.; Ying, S.; Shi, Z. *Polymer* **1998**, *40*, 1341–1345.
- Jo, S.-M.; Lee, W.-S.; Ahn, B.-S.; Park, K.-Y.; Kim, K.-A.; Paeng, I.-S. *R. Polym. Bull. (Berlin)* **2000**, *44*, 1–8.
- Destarac, M.; Matyjaszewski, K.; Silverman, E.; Ameduri, B.; Boutevin, B. *Macromolecules* **2000**, *33*, 4613–4615.
- Gayer, U.; Schuh, T.; Arcella, V.; Albano, M. (Ausimont): EP, 1231239 A1, 2002.
- Valade, D.; Boyer, C.; Ameduri, B.; Boutevin, B. *Macromolecules* **2006**, *39*, 8639–8651.
- Chen, Y.; Sun, W.; Deng, Q.; Chen, L. *J. Polym. Sci., Part A: Polym. Chem.* **2006**, *44*, 3071–3082.
- Ying, L.; Yu, W. H.; Kang, E. T.; Neoh, K. G. *Langmuir* **2004**, *20*, 6032–6040.
- Matyjaszewski, K.; Xia, J. *Chem. Rev.* **2001**, *101*, 2921–2990.
- Wang, J.-S.; Matyjaszewski, K. *Macromolecules* **1995**, *28*, 7901–7910.
- Wang, J.-S.; Matyjaszewski, K. *J. Am. Chem. Soc.* **1995**, *117*, 5614–5615.
- Kato, M.; Kamigaito, M.; Sawamoto, M.; Higashimura, T. *Macromolecules* **1995**, *28*, 1721–1723.
- Percec, V.; Barboiu, B. *Macromolecules* **1995**, *28*, 7970–7972.
- Inceoglu, S.; Olugebefola, S. C.; Acar, M. H.; Mayes, A. M. *Design. Mon. Polym.* **2004**, *7*, 181–189.
- Chen, Y.; Liu, D.; Zhang, N. *Surf. Rev. Lett.* **2005**, *12*, 709–712.
- Chen, Y.; Liu, D.; Deng, Q.; He, X.; Wang, X. *J. Polym. Sci., Part A: Polym. Chem.* **2006**, *44*, 3434–3443.
- Liu, D.; Chen, Y.; Zhang, N.; He, X. *J. Appl. Polym. Sci.* **2006**, *101*, 3704–3712.
- Hester, J. F.; Banerjee, P.; Won, Y. Y.; Akthakul, A.; Acar, M. H.; Mayes, A. M. *Macromolecules* **2002**, *35*, 7652–7661.
- Zhang, M.; Russell, T. P. *Macromolecules* **2006**, *39*, 3531–3539.
- Sauguet, L.; Ameduri, B.; Boutevin, B. Submitted to *Polymer*.
- Pintauer, T.; McKenzie, B.; Matyjaszewski, K. *ACS Symp. Ser.* **2003**, *854*, 130–147.
- Gillies, M. B.; Matyjaszewski, K.; Norrby, P.-O.; Pintauer, T.; Poli, R.; Richard, P. *Macromolecules* **2003**, *36*, 8551–8559.
- Nanda, A. K.; Matyjaszewski, K. *Macromolecules* **2003**, *36*, 1487–1493.
- Nanda, A. K.; Matyjaszewski, K. *Macromolecules* **2003**, *36*, 8222–8224.
- Goodwin, J. M.; Olmstead, M. M.; Patten, T. E. *Abstracts of Papers, 225th ACS National Meeting, New Orleans, LA, March 23–27, 2003*; American Chemical Society: Washington, DC, 2003; POLY-260.
- Kajiwar, A.; Nanda, A. K.; Matyjaszewski, K. *Macromolecules* **2004**, *37*, 1378–1385.
- Kwark, Y.-J.; Novak, B. M. *Macromolecules* **2004**, *37*, 9395–9401.
- Jiang, C.; Zhang, Y. *Chin. J. Chem. Eng.* **2004**, *12*, 208–213.
- Pintauer, T.; Braunecker, W.; Collange, E.; Poli, R.; Matyjaszewski, K. *Macromolecules* **2004**, *37*, 2679–2682.
- Tang, W.; Nanda, A. K.; Matyjaszewski, K. *Macromol. Chem. Phys.* **2005**, *206*, 1171–1177.
- Tang, W.; Matyjaszewski, K. *Abstracts of Papers, 230th ACS National Meeting, Washington, DC, Aug. 28–Sept. 1, 2005*; American Chemical Society: Washington, DC, 2005; POLY-477.
- Matyjaszewski, K.; Nanda, A. K.; Tang, W. *Macromolecules* **2005**, *38*, 2015–2018.
- Kothe, T.; Marque, S.; Martschke, R.; Popov, M.; Fischer, H. *J. Chem. Soc., Perkin Trans. 2* **1998**, 1553–1559.
- Matyjaszewski, K.; Paik, H.-J.; Zhou, P.; Diamanti, S. J. *Macromolecules* **2001**, *34*, 5125–5131.
- Devonport, W.; Michalak, L.; Malmstroem, E.; Mate, M.; Kurdi, B.; Hawker, C. J.; Barclay, G. G.; Sinta, R. *Macromolecules* **1997**, *30*, 1929–1934.
- Wei, M.; Patten, T. E.; Matyjaszewski, K. *Am. Chem. Soc., Polym. Prepr.* **1997**, *38*, 683.
- Shen, X.; He, X.; Chen, G.; Zhou, P.; Huang, L. *Macromol. Rapid Commun.* **2000**, *21*, 1162–1165.
- Woldegiorgis, A.; Loewenhielm, P.; Bjoerk, A.; Roeraade, J. *Rapid Commun. Mass Spectrom.* **2004**, *18*, 2904–2912.
- Guttman, C. M.; Wetzel, S. J.; Flynn, K. M.; Fanconi, B. M.; VanderHart, D. L.; Wallace, W. E. *Anal. Chem.* **2005**, *77*, 4539–4548.
- Yagi, T.; Tatamoto, M. *Polym. J. (Tokyo, Jpn.)* **1979**, *11*, 429–436.
- Russo, S.; Behari, K.; Chengji, S.; Pianca, M.; Barchiesi, E.; Moggi, G. *Polymer* **1993**, *34*, 4777–4781.
- Balague, J.; Ameduri, B.; Boutevin, B.; Caporiccio, G. *J. Fluorine Chem.* **1995**, *70*, 215–223.
- Pianca, M.; Barchiesi, E.; Esposto, G.; Radice, S. *J. Fluorine Chem.* **1999**, *95*, 71–84.
- Guiot, J.; Ameduri, B.; Boutevin, B. *Macromolecules* **2002**, *35*, 8694–8707.

- (59) Guiot, J.; Neouze, M. A.; Sauguët, L.; Ameduri, B.; Boutevin, B. *J. Polym. Sci., Part A: Polym. Chem.* **2005**, *43*, 917–935.
- (60) Boyer, C.; Valade, D.; Sauguët, L.; Ameduri, B.; Boutevin, B. *Macromolecules* **2005**, *38*, 10353–10362.
- (61) Modena, S.; Pianca, M.; Tato, M.; Moggi, G.; Russo, S. *J. Fluorine Chem.* **1989**, *43*, 15–25.
- (62) Ameduri, B.; Boutevin, B.; Kostov, G. *Macromol. Chem. Phys.* **2002**, *203*, 1763–1771.
- (63) Otazaghine, B.; Sauguët, L.; Boucher, M.; Ameduri, B. *Eur. Polym. J.* **2005**, *41*, 1747–1756.
- (64) Kelly, J. Y.; Dominey, R. N.; Resnick, P. R.; DeSimone, J. M. *Prepr. Pap., Am. Chem. Soc., Div. Fuel Chem. Symp.* **2005**, *50*, 575–576.
- (65) Souzy, R.; Ameduri, B.; Boutevin, B. *J. Polym. Sci. Part A: Polym. Chem.* **2004**, *42*, 5077–5097.
- (66) Souzy, R.; Ameduri, B.; Boutevin, B.; Capron, P.; Marsacq, D.; Gebel, G. *Fuel Cells* **2005**, *5*, 383–397.
- (67) Kostov, G.; Ameduri, B.; Sergeeva, T.; Dolbier, W. R., Jr.; W.; R.; Gard, G. L. *Macromolecules* **2005**, *38*, 8316–8326.
- (68) Gelin, M.-P.; Ameduri, B. *J. Fluorine Chem.* **2005**, *126*, 577–585.
- (69) Otazaghine, B.; David, G.; Boutevin, B.; Robin, J. J.; Matyjaszewski, K. *Macromol. Chem. Phys.* **2004**, 154–164.
- (70) Otazaghine, B.; Boyer, C.; Robin, J.-J.; Boutevin, B. *J. Polym. Sci., Part A: Polym. Chem.* **2005**, *43*, 2377–2394.
- (71) Mladenov, G.; Kostov, G.; Ameduri, B.; Mateva, R. *J. Polym. Sci., Part A, Polym. Chem.* **2006**, *44*, 1470–1485.

MA061554A